

hERG K⁺ channel-associated cardiac effects of the antidepressant drug desipramine

Ingo Staudacher · Lu Wang · Xiaoping Wan · Sabrina Obers · Wolfgang Wenzel · Frank Tristram · Ronald Koschny · Kathrin Staudacher · Jana Kisselbach · Patrick Koelsch · Patrick A. Schweizer · Hugo A. Katus · Eckhard Ficker · Dierk Thomas

Abstract Cardiac side effects of antidepressant drugs are well recognized. Adverse effects precipitated by the tricyclic drug desipramine include prolonged QT intervals, torsade de pointes tachycardia, heart failure, and sudden cardiac death. QT prolongation has been primarily attributed to acute blockade of hERG/ I_{Kr} currents. This study was designed to provide a more complete picture of cellular effects associated with desipramine. hERG channels were expressed in *Xenopus laevis* oocytes and human embryonic kidney (HEK 293) cells, and potassium currents were recorded using patch clamp and two-electrode voltage

clamp electrophysiology. Ventricular action potentials were recorded from guinea pig cardiomyocytes. Protein trafficking and cell viability were evaluated in HEK 293 cells and in HL-1 mouse cardiomyocytes by immunocytochemistry, Western blot analysis, or colorimetric MTT assay, respectively. We found that desipramine reduced hERG currents by binding to a receptor site inside the channel pore. hERG protein surface expression was reduced after short-term treatment, revealing a previously unrecognized mechanism. When long-term effects were studied, forward trafficking was impaired and hERG currents were decreased. Action potential duration was prolonged upon acute and chronic desipramine exposure. Finally, desipramine triggered apoptosis in cells expressing hERG channels. Desipramine exerts at least four different cellular effects: (1) direct hERG channel block, (2) acute reduction of hERG surface expression, (3) chronic disruption of hERG trafficking, and (4) induction of apoptosis. These data highlight the complexity of hERG-associated drug effects.

I. Staudacher · S. Obers · K. Staudacher · J. Kisselbach · P. A. Schweizer · H. A. Katus · D. Thomas (✉)
Department of Cardiology,
Medical University Hospital Heidelberg,
Im Neuenheimer Feld 410,
69120, Heidelberg, Germany
e mail: dthomas@ix.urz.uni-heidelberg.de

L. Wang · X. Wan · E. Ficker
Rammelkamp Center, Case Western Reserve University,
MetroHealth Campus,
Cleveland, OH 44109, USA

W. Wenzel · F. Tristram
Institute of Nanotechnology, Karlsruhe Institute of Technology,
76021, Karlsruhe, Germany

R. Koschny
Department of Gastroenterology,
Medical University Hospital Heidelberg,
69120, Heidelberg, Germany

P. Koelsch
Institute of Toxicology and Genetics,
Karlsruhe Institute of Technology,
76021, Karlsruhe, Germany

Keywords Action potential · hERG · Ion channels · K⁺ channel · Long QT syndrome · Torsade de pointes

Introduction

Cardiac action potential repolarization is mainly performed by rapidly and slowly activating components of the delayed rectifier potassium current, I_{Kr} and I_{Ks} . Human ether-a-go-go-related gene (hERG, KCNH2, Kv11.1) K⁺ channels are the molecular counterparts of I_{Kr} (Warmke and Ganetzky 1994; Sanguinetti et al. 1995; Sanguinetti and Tristani-Firouzi 2006). Reduction of hERG currents caused by

mutations produces hereditary long QT syndrome, a potentially lethal cardiac repolarization disorder. Furthermore, excessive drug-induced blockade of hERG channels underlies acquired long QT syndrome, a frequent finding associated with characteristic ventricular “torsade de pointes” arrhythmias and sudden cardiac death (Viskin 1999; Redfern et al. 2003; Thomas et al. 2003, 2006; Morita et al. 2008; Roden 2008). I_{Kr} reduction may be caused by dual mechanisms, acute inhibition of hERG channels and chronic drug-induced disruption of hERG protein trafficking into the cell surface membrane (Ficker et al. 2004; Cordes et al. 2005; Kuryshev et al. 2005; Wible et al. 2005; Rajamani et al. 2006; Thomas et al. 2006; Guo et al. 2007; Takemasa et al. 2007; Wang et al. 2007; Van der Heyden et al. 2008; Obers et al. 2010; Staudacher et al. 2010). In addition to cardiac tissue, hERG potassium channels are expressed in tumor cells where they are involved in the regulation of cell proliferation and apoptosis (Bianchi et al. 1998; Cherubini et al. 2000; Smith et al. 2002; Wang et al. 2002; Crociani et al. 2003). Initiated by these observations, a third mechanism leading to hERG-associated adverse effects was recently revealed. Inhibition of cardiac hERG channels by the antihypertensive drug doxazosin, which is associated with increased incidence of heart failure (ALLHAT Study 2000), promotes apoptosis in human embryonic kidney (HEK 293) cells (Thomas et al. 2004a, 2008). Thus, hERG-related apoptosis may represent a process contributing to heart failure in patients treated with doxazosin and other hERG inhibitors.

hERG-linked adverse effects represent a significant cardiovascular liability of clinical and developmental drugs. Tricyclic antidepressant agents are particularly notorious for their association with acquired long QT syndrome, life-threatening ventricular arrhythmias, and heart failure, which may be precipitated or aggravated by heart disease, drug overdose, or in elderly patients (Coccaro and Siever 1983; Witchel et al. 2003). As depression is often associated with suicide, cardiovascular safety of antidepressant drugs should be as high as possible. The dissection of molecular mechanisms that underlie the cellular effects of hERG blockers improves risk assessment of drugs and may serve to optimize preclinical safety screens during pharmaceutical research and development. Desipramine is a tricyclic drug that is used to treat depression, attention deficit disorder, neuropathic pain, and cocaine or opiate withdrawal. Cardiac safety concerns have been raised by reports on QT interval prolongation, ventricular torsade de pointes tachycardia, and cases of sudden death (Cosazza et al. 1986; Alderton 1995; Leonard et al. 1995; Swanson et al. 1997; Waslick et al. 1999; Varley 2001). In addition, cardiotoxicity has been linked to the compound; however, this potential side effect appears to be rare (Burckhardt et al. 1978; Glassmann et al. 1983; Dietrich et al. 1993). In addition to adverse cardiac

actions, desipramine has been associated with beneficial antiarrhythmic effects. In rat models of acute myocardial ischemia, application of desipramine reduced the incidence of ventricular arrhythmias (Daugherty et al. 1986; Kurz et al. 1995; Du et al. 1998). This antiarrhythmic effect has been attributed in part to inhibition of endogenous norepinephrine release by the drug.

This study was designed to investigate drug actions on hERG currents, hERG protein surface expression, and hERG-associated apoptosis. Using desipramine as a prototype antidepressant drug, four different mechanisms of hERG-associated cellular effects are revealed. First, acute electrophysiological effects of desipramine on recombinant hERG channels and on cardiac action potentials recorded in guinea pig ventricular myocytes were investigated. Second, reduction of hERG surface protein by short-term application of desipramine was observed, revealing a novel biochemical mechanism of drug-induced acute QT prolongation. Third, the molecular basis of chronic effects associated with desipramine treatment was assessed by measuring hERG protein trafficking and action potential prolongation upon long-term drug exposure. Finally, apoptosis was demonstrated in hERG-expressing cells treated with desipramine.

Methods

Molecular biology

Procedures for in vitro transcription and oocyte injection were performed as published previously (Kiehn et al. 1999). Mutations in hERG wild type (WT; GenBank accession number: NM 000238) and hERG WT HA_{ex} with an extracellular hemagglutinin (HA) tag (Ficker et al. 2004) described in the text were introduced using the QuikChange Site-Directed Mutagenesis kit (Stratagene, La Jolla, CA, USA) and synthetic mutant oligonucleotide primers. All complementary DNA (cDNA) constructs were confirmed by DNA sequencing. Complementary RNAs (cRNAs) were transcribed after vector linearization using SP6 RNA polymerase and the mMessage mMachine kit (Ambion, Austin, TX, USA). Transcripts were quantified using a spectrophotometer and by comparison with control samples separated by agarose gel electrophoresis, and 46 nl cRNA encoding study channels was injected into stage V–VI defolliculated *Xenopus* oocytes. The investigation conforms to the *Guide for the Care and Use of Laboratory Animals* published by the U.S. National Institutes of Health (NIH publication No. 86-23, revised 1996). All experiments followed the European Community guidelines for the use of experimental animals. This study has been approved by a local Ethics Board (reference number A-19/07).

Cell culture

cDNA encoding the hERG WT potassium channel cloned in pCDNA3 was stably transfected into the human embryonic kidney cell line HEK 293 as described (Ficker et al. 2003, 2004; Thomas et al. 2001). Transient transfections of hERG F656V, hERG WT HA_{ex}, and hERG F656V HA_{ex} cDNAs (in pcDNA3) into HEK 293 cells were performed using Fugene 6 transfection reagent (Roche Diagnostics, Indianapolis, IN, USA) according to the manufacturer's instructions. Cells were cultured in Dulbecco's Modified Eagle Medium (Gibco BRL, Rockville, IL, USA; electrophysiology and biochemistry) or minimum essential medium (Gibco BRL; cell viability assays) supplemented with 10% fetal bovine serum (FBS), 2 mM L-glutamine, 100 U/ml penicillin G sodium, 100 µg/ml streptomycin sulfate, and 500 µg/ml geneticin (G418; all from Gibco BRL) in an atmosphere of 95% humidified air and 5% CO₂ at 37°C. For transiently transfected and non-transfected cells, geneticin was omitted from the culture media. Cells were passaged regularly and subcultured prior to treatment. For biochemical analyses, drugs were added prior to Western blot analyses as indicated.

The HL-1 cardiomyocyte cell line was established by Dr. Claycomb (Claycomb et al. 1998). HL-1 cells were plated on culture dishes coated with gelatin and fibronectin (both from Sigma-Aldrich) and maintained at 37°C in an atmosphere of 95% humidified air and 5% CO₂ in Claycomb medium (Sigma-Aldrich) supplemented with 10% FBS, 2 mM L-glutamine, 0.1 mM norepinephrine (Sigma-Aldrich), penicillin, and streptomycin as published (Claycomb et al. 1998). The medium was changed approximately every 24–48 h. When confluence was reached, cells were dissociated using 0.05% trypsin/ethylenediaminetetraacetic acid (EDTA) (Gibco BRL) and resuspended in complete Claycomb medium at a density of 25 × 10⁶ cells/60 mm dish for Western blotting and at a density of 25,000 cells/gelatin–fibronectin-coated coverslip for electrophysiological recordings.

Drugs

Desipramine (Sigma-Aldrich, Steinheim, Germany) was prepared as 10 mM stock solution in H₂O (*Xenopus* oocyte studies) or dimethylsulfoxide (DMSO; HEK cell studies). E4031 (Sigma-Aldrich) was prepared as 10 mM stock solution in H₂O. Pentamidine (Sigma-Aldrich) was dissolved in H₂O to a 30 mM stock solution. Astemizole, doxazosin, and nisoldipine (all from Sigma-Aldrich) were prepared as 10 mM stock solution in DMSO. Final DMSO concentrations in drug-containing solutions did not exceed 0.1%. Aliquots of the stock solutions were diluted freshly

to the desired concentrations with bath solution or culture media, respectively, on the day of experiments.

Electrophysiology

Two-electrode voltage clamp measurements were performed as described (Thomas et al. 1999). Whole cell currents were measured 2 to 4 days after injection with an Oocyte Clamp amplifier (Warner Instruments, Hamden, CT, USA). Electrodes were filled with 3 M KCl and had tip resistances of 1–5 MΩ. Recordings were performed under constant perfusion at room temperature. Voltage clamp measurements of *Xenopus* oocytes were performed in a solution containing (in mM): 5 KCl, 100 NaCl, 1.5 CaCl₂, 2 MgCl₂, and 10 4-(2-hydroxyethyl)-1-piperazineethanesulfonic acid (HEPES; pH adjusted to 7.4 with NaOH). Current and voltage electrodes were filled with 3 M KCl solution. Data were sampled at 2 kHz and filtered at 1 kHz.

Current recordings from HEK 293 cells and from HL-1 cardiac myocytes were carried out using the whole cell patch clamp configuration as reported earlier (Thomas et al. 2001). Patch clamp electrodes were filled with the following solution (in mM): 100 K-aspartate, 20 KCl, 2.0 MgCl₂, 1 CaCl₂, 10 EGTA, and 10 HEPES (pH adjusted to 7.2 with KOH). The external solution contained (in mM): 140 NaCl, 5.0 KCl, 1.0 MgCl₂, 1.8 CaCl₂, 10 HEPES, and 10 glucose (pH adjusted to 7.4 with NaOH). During recordings from HL-1 cells, L-type Ca²⁺ currents were blocked with 1 µM nisoldipine. To analyze current densities, membrane capacitance was measured using the analogue compensation circuit of the patch clamp amplifier.

Cardiac action potentials were recorded from freshly isolated ventricular guinea pig myocytes and in myocytes kept in short-term culture using the perforated patch technique to preserve the intracellular milieu of the intact cardiomyocyte. Isolation of guinea pig ventricular myocytes was carried out as described (Ficker et al. 2003). Cardiac myocytes were cultured in M199 medium (Gibco BRL) in an atmosphere of 95% humidified air and 5% CO₂ at 37°C. Patch pipettes were back-filled with (in mM): 120 K-aspartate, 20 KCl, 10 NaCl, 2.0 MgCl₂, and 5 HEPES (pH adjusted to 7.3 with KOH), supplemented with 240 µg/ml amphotericin-B (Sigma). The extracellular solution was Tyrode's solution (137 mM NaCl, 5.4 mM KCl, 2 mM CaCl₂, 1 mM MgSO₄, 10 mM glucose, and 10 mM HEPES, pH 7.3). Following seal formation, access resistance was continuously monitored. Experimental protocols were initiated after the access resistance dropped below 40 MΩ. Action potentials were elicited in current clamp mode at a stimulation frequency of 0.5 Hz and recorded at near physiological temperatures of 30–32°C. To study long-term drug effects on cardiac action potentials, desipramine and E4031 were added overnight prior to recordings as indicated.

E4031 (5 μ M) was used to specifically block cardiac I_{Kr} currents in guinea pig cardiomyocytes.

Experiments were carried out at room temperature (20–22°C), and no leak subtraction was done during the experiments. PCLAMP (Molecular Devices, Sunnyvale, CA, USA) and Origin (OriginLab, Northampton, MA, USA) software were used for data acquisition and analysis in all electrophysiological experiments.

Western blot analysis

Immunodetection of hERG protein was performed by sodium dodecyl sulfate (SDS) gel electrophoresis and Western blotting. Antibodies used in the present study have been described previously (Ficker et al. 2003, 2004). HEK-hERG and HL-1 cells were solubilized for 1 h at 4°C in lysis buffer containing 1% Triton X-100 and “Complete” protease inhibitors (Roche Diagnostics, Indianapolis, IN, USA). Protein concentrations were determined with the BCA method (Pierce, Rockford, IL, USA). Proteins were then separated on SDS polyacrylamide gels, transferred to polyvinylidene difluoride membranes, and detected using rabbit anti-hERG polyclonal antibody (hERG 519; Ficker et al. 2003; HEK 293 cells), rabbit anti-erg1 polyclonal antibody (APC-016; Alomone Labs, Jerusalem, Israel; HL-1 cells), and mouse monoclonal anti-actin antibody (A4700; Sigma Aldrich). ECL Plus reagent (GE Healthcare, Piscataway, NJ, USA) was used for signal development.

Chemiluminescence detection of cell surface hERG protein

For chemiluminescence detection, HEK cells were transiently transfected with hERG WT HA_{ex} or HEK-hERG F656V HA_{ex} cDNA and treated with desipramine or pentamidine. Labeling with anti-HA and HRP-conjugated secondary antibodies allowed for ready detection of hERG surface protein. HEK cells were plated at 25,000 cells/well in 96-well plates coated with ECL cell attachment matrix (0.1 mg/ml, overnight at 4°C; Upstate, Lake Placid, NY, USA) and transiently transfected with 50 ng/well of either HEK-hERG WT HA_{ex} or HEK-hERG F656V HA_{ex} cDNA using Fugene transfection reagent (Roche Diagnostics). Twenty-four hours after transfection, cells were incubated for 30, 60, or 120 min, or overnight (16–20 h) with desipramine or pentamidine as indicated. Following drug application, cells were fixed, blocked, and incubated for 1 h with rat anti-HA-monoclonal antibody (clone 3F10, Roche Diagnostics). After washing, HRP-conjugated goat anti-rat IgG (Jackson ImmunoResearch Laboratories Inc, West Grove, PA, USA) and the double-stranded DNA stain SYBR Green I (Invitrogen, Carlsbad, CA, USA) were added for 1 h before SYBR Green fluorescence was measured to determine cell number (Wible et al. 2005).

Chemiluminescent signals were developed using SuperSignal (Pierce) and captured in a Beckman Coulter DTX 880 plate reader (Beckman Coulter, Fullerton, CA, USA). Luminescence signals were corrected for cell loss as measured by SYBR Green fluorescence with the data presented as normalized surface expression relative to control.

Immunocytochemistry and confocal imaging

HEK-hERG cells were grown overnight on poly-lysine-coated glass coverslips or chamber slides under control conditions or in the presence of 30 μ M desipramine. Following incubation, cells were washed with phosphate-buffered saline (PBS) and fixed in ice cold 4% formaldehyde/PBS for 30 min. After fixation, cells were washed, permeabilized with 0.1% Triton X-100, and blocked in 5% goat serum/PBS for 30–60 min at room temperature. For double labeling, permeabilized cells were incubated overnight at 4°C with rabbit anti-hERG GST antibody (1:100; Alomone Labs, Jerusalem, Israel) and mouse anti-KDEL antibody (1:100; Stressgen Biotechnology, Collegeville, PA, USA). The tetrapeptide KDEL, located at the carboxy-terminal sequences of luminal proteins, is a retrieval motif essential for sorting of these proteins along the secretory pathway. KDEL proteins perform essential functions in the endoplasmic reticulum (ER) related to protein folding and assembly. The antibody used in this study has been raised against a six residue synthetic peptide (SEKDEL) conjugated to keyhole limpet hemocyanin. Primary antibodies were washed off using PBS. Cells were then re-blocked in 5% goat serum (30 min) and incubated for 2 h at room temperature with secondary anti-rabbit FITC (1:100; Jackson Labs, Bar Harbor, ME, USA) and anti-mouse Rhodamine RedX antibody (1:100, Jackson Labs). After a final wash in PBS, coverslips were mounted with Vectashield and examined using a Leica laser scanning confocal microscope (Leica, Solms, Germany).

Immunodetection of cleaved PARP

For immunodetection of cleaved poly-ADP-ribose-polymerase (PARP; Obers et al. 2010), HEK and HEK-hERG cells were cultured for 5.5 h in the absence or presence of hERG desipramine (25 μ M) or doxazosin (30 μ M), respectively. HEK and HEK-hERG cells were then fixed with formalin, embedded in paraffin, cut into 3 μ m sections, de-waxed, and rinsed with PBS. Sections were blocked (20 min) with PBS solution containing 20 mg/ml bovine serum albumin (Serva Biochemicals, Heidelberg, Germany) and 1 mg/ml human γ -globulin (Gamma-Venin; Aventis-Behring, Marburg, Germany). For double labeling, cells were incubated for 1 h at room temperature with rabbit anti-cleaved PARP antibody (1:100; Abcam, Cambridge,

MA, USA) and mouse anti-CD326 antibody (1:200; Chemicon International; Temecula, CA, USA) in blocking solution. Specificity of antibody labeling was assessed by substituting primary antibodies with mouse (1:10; Dako Cytomation, Glostrup, Denmark) and rabbit isotype control antibodies (1:10; Invitrogen) (data not shown). Primary antibodies were washed off using PBS. Cells were re-blocked in 20% normal goat serum (Dianova, Hamburg, Germany) (20 min) and incubated for 30 min at room temperature with secondary antibodies (1:100 dilution; goat anti-rabbit Alexa Fluor 488 and goat anti-mouse Alexa Fluor 568; Invitrogen). After removal of secondary antibodies, sections were briefly (5 s) treated with 4',6-diamidino-2-phenylindole (DAPI; 1 µg/ml in PBS) and rinsed. Coverslips were mounted with FluorSave Reagent (Calbiochem, La Jolla, CA, USA) and examined using an Olympus fluorescence microscope (AX 70; Olympus, Hamburg, Germany).

MTT cell viability assay

The colorimetric MTT (3-(4,5-dimethylthiazol-2-yl)-2,5-diphenyl tetrazolium bromide) assay was used to quantify cell viability. MTT is cleaved by living, metabolically active cells, resulting in reduction of yellow MTT to a dark blue formazan product allowing for ready detection and quantification (Mosmann 1983). The assay was carried out as published previously (Obers et al. 2010). A total of 12,000 HEK or HEK-hERG cells, respectively, were seeded in 96-well plates (Costar, Cambridge, MA, USA) in 100 µl medium per well at 37°C. After 24 h, the medium was removed and respective hERG inhibitors (50 µM desipramine or 30 µM doxazosin) in 100 µl culture media were added. Control cells were cultured in medium without additional drugs, representing 100% cell viability. To define 0% viability, a group of cells were lysed completely in Triton-X (1% in PBS). Following treatment (22 h), 30 µl MTT solution (2.5 mg/ml in PBS; Sigma-Aldrich) was added for 4 h. Finally, the medium was removed and cells were lysed in a 95% isopropanol/5% acetic acid solution (v/v), before absorption was determined at 560 nm using a spectrophotometer. Three wells were measured for each single experiment, and the percentage of viable cells was calculated according to: $100 \times [\text{absorption measured} - (\text{absorption of lysed cells} + \text{blank measurement})] / [\text{absorption of medium} - (\text{absorption lysed cells} + \text{blank measurement})]$.

Molecular modeling

The crystal structure of the KvAP (voltage-dependent potassium channel from *Aeropyrum pernix*; PDB ID 1ORQ; Jiang et al. 2003) served as template for a three-dimensional homology model of the hERG K⁺ channel

pore region. The model comprising the hERG S5, pore, and S6 domains was created using Prime (Farid et al. 2005). We then used FlexScreen, a virtual screening program to perform receptor–ligand docking simulations in an atomistic representation of the protein and the ligand (Merlitz and Wenzel 2002; Merlitz et al. 2003). The FlexScreen scoring function is based on adaptable biophysical models, including a solvation contribution (Eisenberg and McLachlan 1986; Jorgensen and McDonald 1997; Morris et al. 1998). Desipramine was docked using a cascaded version of a stochastic tunneling algorithm which samples translations of the center-of-mass and rotations of the ligand, as well as intra-molecular conformational changes (Wenzel and Hamacher 1999). In addition to the degrees of freedom of the ligand, receptor conformational change is accounted for in selected regions of the protein backbone and selected side chains (Kokh and Wenzel 2008). An optimized docked conformation is shown in Fig. 1f, g. Previous work demonstrated that this approach yields accurate results for binding mode prediction and improves selectivity in library screens for a number of pharmaceutically relevant receptors (Fischer et al. 2007; Kokh and Wenzel 2008).

Data analysis

Concentration–response relationships for drug-induced block were fit with a Hill equation of the following form: $I_{\text{drug}}/I_{\text{control}} = 1/[1 + (D/IC_{50})^n]$, where I indicates current or image density, D is the drug concentration, n is the Hill coefficient, and IC_{50} is the concentration necessary for 50% block. When concentration-dependent restoration of hERG trafficking was assessed, IC_{50} was replaced by EC_{50} to indicate the concentration required for half-maximal effect. Activation and inactivation curves were fit with a single-power Boltzmann distribution of the form $I_{\text{tail}} = I_{\text{tail,max}} / [1 + e^{(V_{1/2} - V)/k}]$, where V is the test pulse potential, $V_{1/2}$ is the half-maximal activation/inactivation potential, and k is the slope of the activation curve.

Statistics

Data are expressed as mean ± SEM of n experiments or cells studied. We used paired and unpaired Student's t tests (two-tailed tests) to compare the statistical significance of the results: $P < 0.05$ was considered statistically significant. Multiple comparisons were performed using one-way ANOVA. If the hypothesis of equal means could be rejected at the 0.05 level, pair-wise comparisons of groups were made and the probability values were adjusted for multiple comparisons using the Bonferroni correction. To compare data presented in Fig. 8b, c, ANOVA was followed by a two-tailed Dunnett's test.

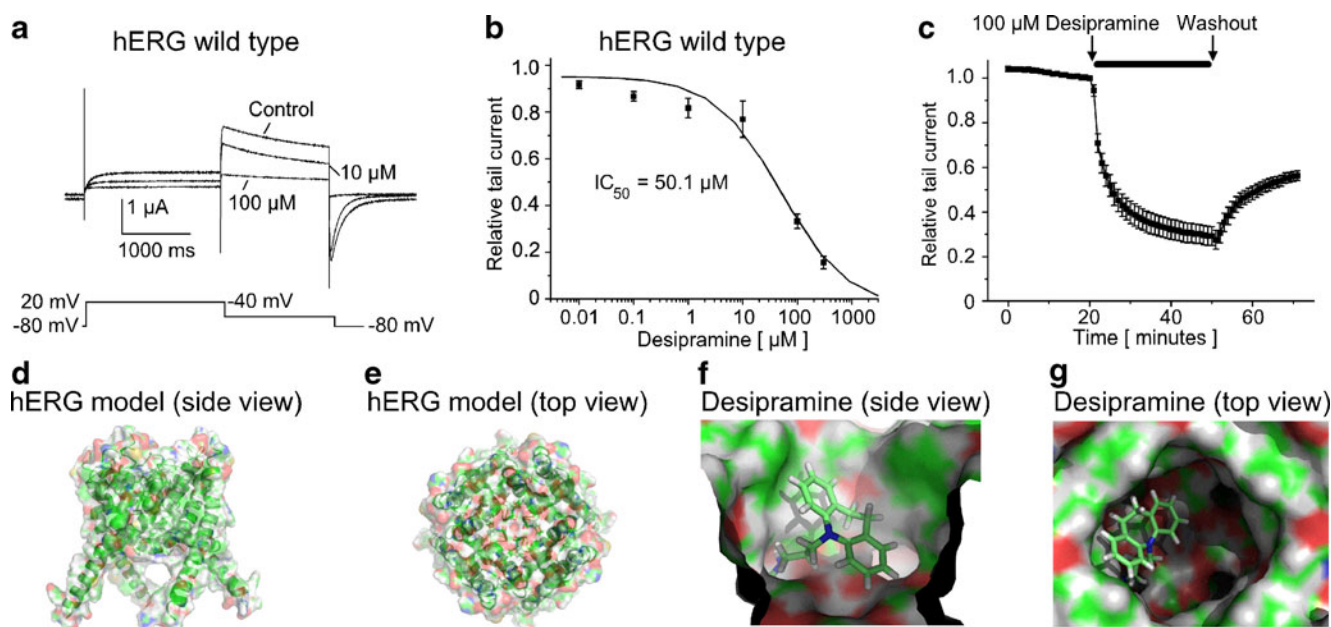


Fig. 1 Acute pore blockade of hERG K⁺ channels by the antidepressant drug desipramine. **a** hERG current traces recorded after heterologous expression in *Xenopus* oocytes under control conditions and after application of 10 and 100 μM desipramine are shown. **b** Corresponding concentration response relationship, revealing an IC₅₀ value of 50.1 μM ($n=4$ 13 cells studied). **c** Time course of acute hERG tail current blockade by 100 μM desipramine ($n=7$). Note that, for the purpose of clear presentation, not all current measurements are displayed. Data are expressed as mean ± SEM. **d, e** Homology model for the hERG pore region, based on the crystal structure of the KvAP potassium channel. *Ribbon diagrams* with additional surface representation are shown from the *side* (**d**) and from the *top* (**e**), with the

extracellular solution *above* and the intracellular space *below*. Four subunits of the channel (including S5, pore, and S6 domains) are colored uniquely. Aromatic side chains of residues Y652 and F656 are shown as *sticks*. **f, g** Docking model of a desipramine molecule within the hERG pore cavity. Close up *side* (**f**) and *top* (**g**) views in the four subunit model of the channel (**d, e**) are shown, respectively. Surface representation of the channel pore region is colored to highlight the location of acidic, negative charges (*red*) and of basic, positive charges (*blue*). The figure was generated using PyMol (DeLano Scientific; San Carlos, CA, USA) on the basis of the docking simulations described in the text

Results

Acute inhibition of hERG potassium channels by desipramine

Desipramine directly blocked hERG channels expressed in *Xenopus laevis* oocytes in a concentration-dependent fashion (Fig. 1). Currents were elicited by a 2-s depolarizing step to +20 mV followed by a repolarizing step to -40 mV for 1.6 s to produce slowly decaying outward tail currents. The holding potential was -80 mV in all experiments performed in this study, unless indicated otherwise. Pulses were applied at a frequency of 0.1 Hz during superfusion with the drug solution for 30 min. After the monitoring period, the degree of block was determined (Fig. 1a). To study the concentration dependence of hERG current block by desipramine, peak tail currents in the presence of the drug were normalized to the respective control values and plotted as relative current amplitudes in Fig. 1b ($n=4$ to 13 oocytes were investigated at each concentration). The half-maximal inhibitory concentration (IC₅₀) for block of tail currents yielded 50.1±19.4 μM with a Hill coefficient n_H of 0.71±0.16. The time course of block is shown in Fig. 1c ($n=7$).

After a control period of 20 min, hERG channel block by 100 μM desipramine reached steady-state conditions after 30 min. Upon washout (20 min), the blocking effects of desipramine on hERG were partially reversible.

Computational modeling of hERG–desipramine interactions

We used FlexScreen all-atom receptor–ligand docking software to dock desipramine into a KvAP-based homology model of hERG (Merlitz and Wenzel 2002; Merlitz et al. 2003) (Fig. 1d, e). This *in silico* approach confirmed the significance of aromatic pore residues for the hERG–desipramine interaction. The results of these simulations (Fig. 1f, g) demonstrate that the extended methylamine group of the molecule fits into the pore cavity of the channel, while the aromatic rings coordinate with the hydrophobic side chains of Y652 and F656. Corresponding to the data presented in Fig. 5b and to the results reported by Hong et al. (2010), this model is consistent with reduced desipramine binding affinity caused by mutation of Y652 or F656 residues, leading to alteration of size and/or shape of the drug-binding pocket.

The biophysical mechanism of acute hERG current inhibition by desipramine

To investigate whether the channel is blocked in the closed or activated (i.e., open and/or inactivated) state, we activated currents using a protocol with a single depolarizing step to 0 mV for 7.5 s. Following control measurements, we allowed 100 μM of the drug to wash in for 30 min while holding the channels in the closed state at -80 mV before measurements with desipramine were performed (Fig. 2a). The degree of inhibition (i.e., $(1 - \text{current in the presence of desipramine}/\text{control current}) \times 100$) is displayed in Fig. 2b. Analysis of the test pulse after desipramine application revealed a time-dependent increase of block to 75.6% at 1,000 ms in this representative cell (Fig. 2b), which is consistent with block of activated hERG potassium channels. In this series of experiments, 100 μM desipramine reduced hERG outward currents at the end of the 0-mV pulse by $75.4 \pm 4.5\%$ ($n=6$).

To address the question whether hERG channels are also blocked in the inactivated state, a long inactivating test pulse to $+80$ mV (4 s) was applied, followed by a second voltage step (0 mV, 3.5 s) to open hERG channels ($n=8$). Typical current traces under control conditions and after application of 100 μM desipramine for 30 min while holding the cell at -80 mV are displayed in Fig. 2c. Figure 2d depicts normalized relative block upon channel opening during the second voltage pulse (0 mV). We observed time-dependent onset of open channel block, suggesting that inactivated hERG channels were not targeted by desipramine during the preceding $+80$ -mV pulse. Currents at the end of the second voltage step (0 mV) were reduced by $63.2 \pm 3.1\%$ ($n=8$). We conclude from these experiments that desipramine inhibits hERG channels predominantly in the open state.

Frequency dependence of desipramine block

Frequency dependence of block was investigated using the following approach. hERG potassium channels were rapidly activated by a depolarizing step to 20 mV for 300 ms, followed by a repolarizing step to -40 mV (300 ms) to elicit outward tail currents. Pulses were applied at intervals of 1 or 10 s under control conditions and in the presence of 30 μM desipramine, with each cell studied only at one stimulation rate. The development of current reduction was plotted versus time (Fig. 2e), and the resulting level of steady-state block served as a measure of the frequency dependence of block. The degree of steady-state inhibition at 1 Hz ($33.2 \pm 1.9\%$; $n=3$) was significantly higher compared to 0.1 Hz ($16.7 \pm 3.6\%$, $n=5$), illustrating frequency dependence of block.

Effects of desipramine on hERG current activation

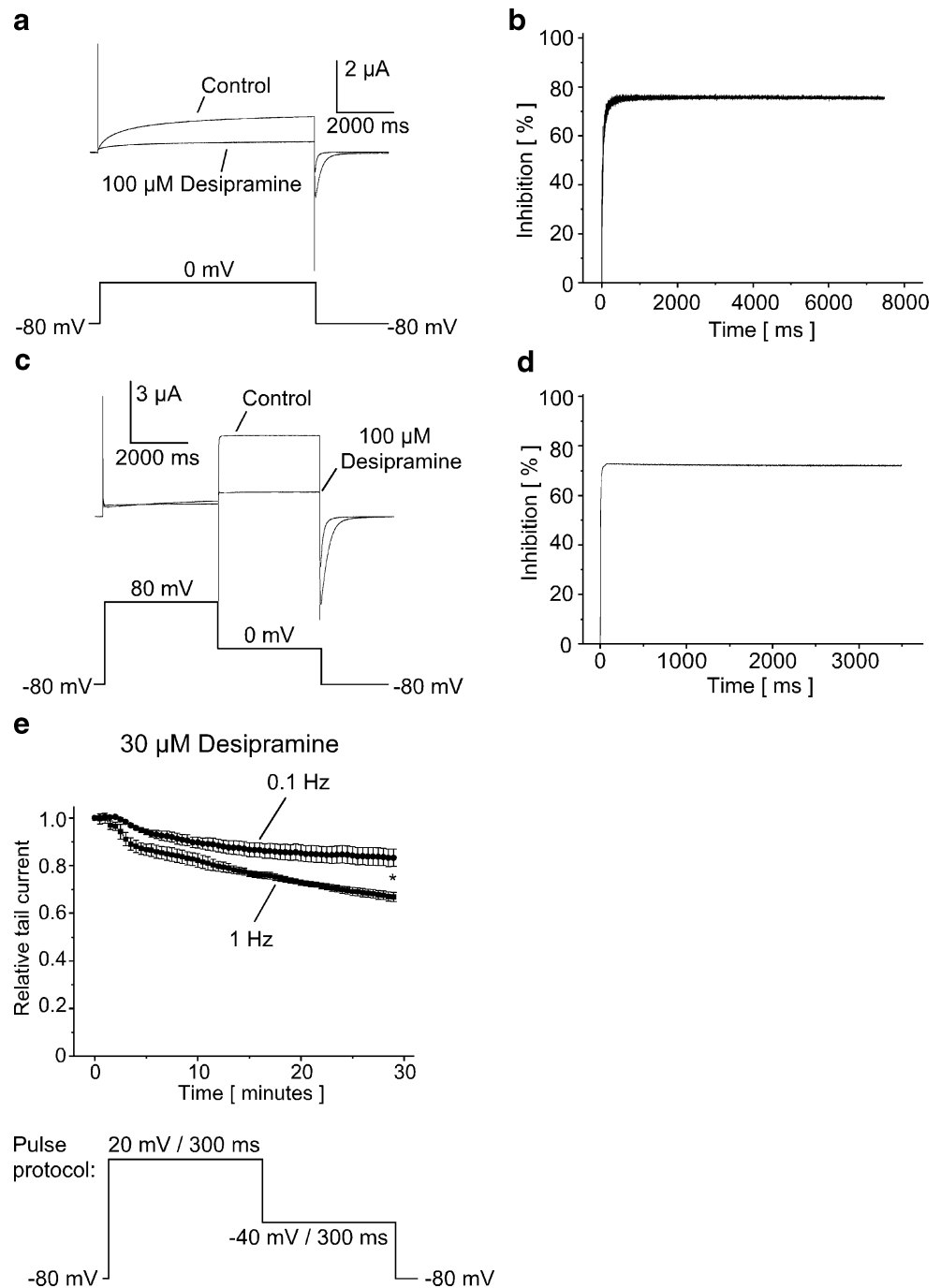
The effect of desipramine on hERG current–voltage (I – V) relationship was investigated in *Xenopus* oocytes under isochronal recording conditions. Depolarizing pulses were applied for 2 s to voltages between -80 and $+70$ mV in 10 mV increments (0.2 Hz), and tail currents were recorded during a constant repolarizing step to -60 mV for 1.6 s. Families of current traces from one cell are shown for control conditions and after exposure to 30 μM desipramine (30 min) (Fig. 3a, b). Currents activated at potentials greater than -60 mV, reached a peak at -10 mV and then decreased at more positive potentials due to inactivation (Sanguinetti et al. 1995), giving the I – V relationship a bell-shaped appearance (Fig. 3c, d). Panels e and f of Fig. 3 display activation curves (i.e., peak tail currents as a function of the preceding test pulse potential). hERG currents at the end of the test pulse to -10 mV were reduced by $36.7 \pm 4.7\%$, and peak tail currents were blocked by $44.1 \pm 10.3\%$ ($n=3$). The half-maximal activation voltage was not significantly affected ($V_{1/2, \text{control}} = -16.6 \pm 3.5$ mV; $V_{1/2, \text{desipramine}} = -17.3 \pm 3.0$ mV; $n=3$).

Desipramine does not affect hERG channel inactivation

Desipramine effects on hERG current inactivation were investigated using two approaches. First, it was tested whether the time constant of inactivation was affected by the drug. Pulses to 40 mV were applied for 900 ms, where channels are predominantly inactivated. Brief repolarizations to -100 mV for 16 ms caused rapid recovery from inactivation without marked deactivation. During a second depolarizing pulse (150 ms) to different voltages ranging from -40 to 40 mV (increment 20 mV), rapidly inactivating currents were produced. Inactivating currents were recorded in the absence of the drug (Fig. 4a) and after equilibration of block with 30 μM desipramine (Fig. 4b) by current monitoring for 30 min as described. As the inactivation time constant depends on the current magnitude, a set of control cells and matching oocytes after desipramine application with similar mean current amplitudes at the end of the 40-mV pulse (0.26 ± 0.01 μA versus 0.26 ± 0.01 μA) were compared. Single exponential fits to large inactivating currents yielded the time constants of inactivation at different voltages. There was a tendency towards accelerated inactivation in the presence of desipramine (Fig. 4c; $n=5$ oocytes were analyzed in each series). However, this effect was not statistically significant.

To measure steady-state inactivation relationships, channels were inactivated at a holding potential of 20 mV, followed by recovery from inactivation for 20 ms at potentials from -120 to 30 mV (increment 10 mV). The resulting peak outward currents at constant 20 mV were

Fig. 2 Block of open hERG channels by desipramine. **a, b** After having recorded the control measurement, the oocyte was clamped at 80 mV for 30 min during superfusion with the drug solution (100 μ M desipramine). The control recording and the first pulse measured after the incubation period are displayed (**a**). **b** The degree of activated channel inhibition in percent. Current inhibition increased time dependently to ~76% at 1,000 ms in this representative experiment. **c, d** Inactivated channels are insensitive to desipramine. hERG channels were inactivated by a first voltage step to +80 mV, followed by channel opening at 0 mV. The corresponding relative block during the 0 mV step is displayed in **d**. Time dependent development of block upon channel opening during the second voltage step is illustrated, indicating that little or no inhibition occurred in the inactivating state during the first step. **e** Frequency dependence of hERG channel block by desipramine. Mean relative tail current amplitudes (1 and 0.1 Hz stimulation rate, $n=3$ and five oocytes studied, respectively) are plotted versus time ($*P < 0.05$). For the purpose of clear presentation, not all measurements are displayed



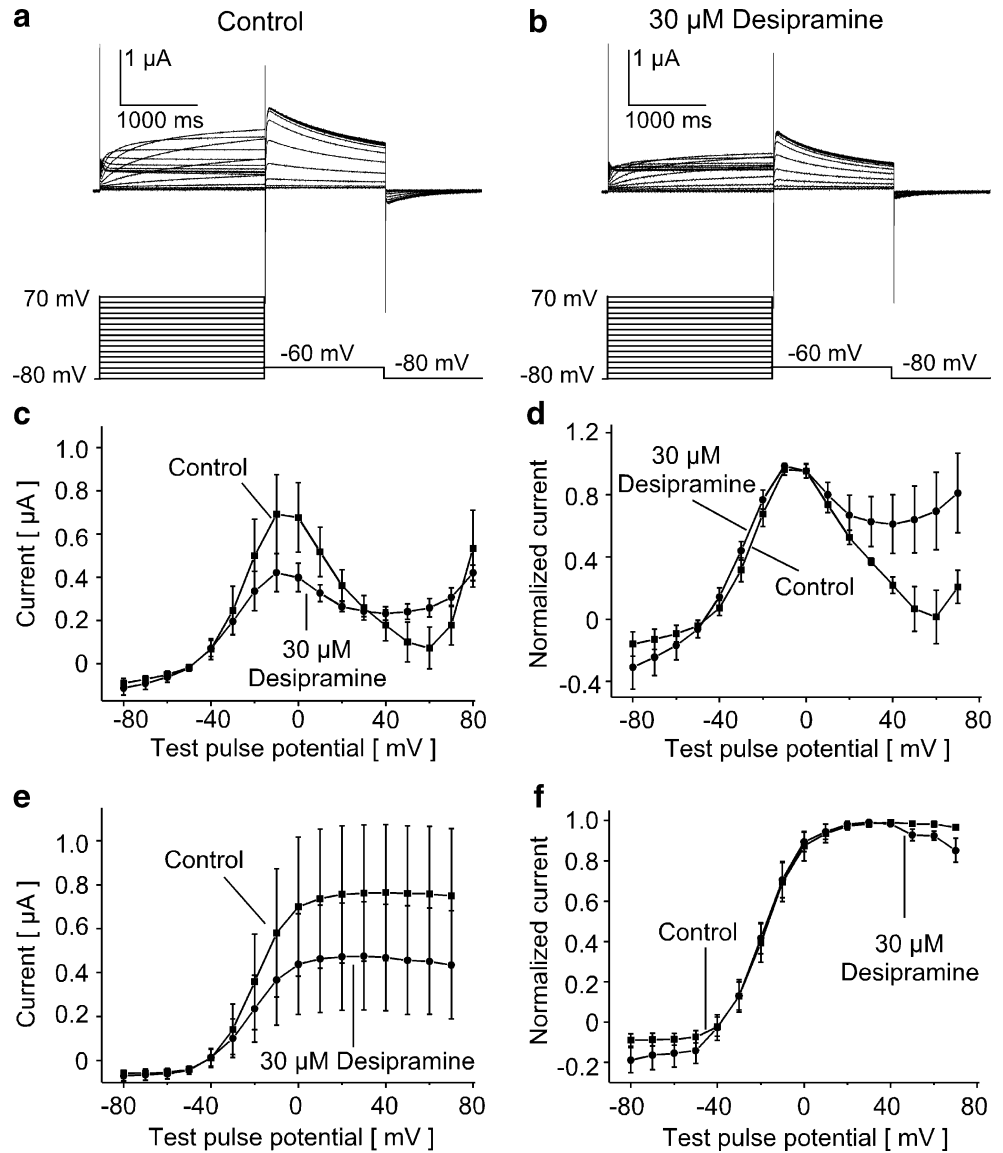
analyzed as measure of steady-state inactivation. After recording control measurements (Fig. 4d), 30 μ M desipramine was applied. The holding potential was -80 mV during current monitoring for 30 min to avoid destruction of the cell that occurs when holding the cell at 20 mV. A typical recording in the presence of the drug is displayed in Fig. 4e. The inactivating outward current amplitudes measured at 20 mV were normalized and plotted versus test pulse potentials, revealing that steady-state inactivation was not significantly affected by desipramine ($V_{1/2,control} =$

-67.0 ± 2.8 mV; $V_{1/2,desipramine} = -63.9 \pm 3.9$ mV; $n=5$; Fig. 4f).

Desipramine blocks hERG currents and reduces surface protein levels in a human cell line

To study acute desipramine block of hERG in mammalian cells, we expressed hERG potassium channels stably in HEK 293 cells. Channels were activated by a 2-s depolarization to +20 mV, and outward tail currents were

Fig. 3 Voltage dependence of hERG activation. Control measurement (a) and the effect of 30 μ M desipramine (30 min; b) are shown. c, d Mean current amplitudes at the end of the test pulse as function of the preceding test pulse potential under control conditions and after incubation with desipramine (c, original current amplitudes; d, values normalized to maximum step currents) ($n=3$). e, f Activation curves, i.e., peak tail current amplitudes as function of the preceding test pulse potential during the first step of the voltage protocol (e, original current amplitudes; f, values normalized to peak tail currents) ($n=3$). The mean half maximal activation potential $V_{1/2}$ was not significantly affected by desipramine



recorded during a step to -50 mV for 2 s (Fig. 5a). During wash-in of the drug, we applied this protocol at 0.1 Hz frequency until steady-state block was maintained for at least 30 s. hERG currents were blocked by desipramine in a concentration-dependent manner. The IC_{50} value for desipramine block of hERG tail currents was 11.9 ± 1.9 μ M with a Hill coefficient n_H of 1.01 ± 0.14 (Fig. 5b; $n=3-8$ cells were studied at each concentration). Drug affinity was reduced in HEK 293 cells by substitution of aromatic residue F656 by a non-aromatic amino acid (valine). The IC_{50} value for hERG F656V inhibition by desipramine yielded 48.3 ± 22.0 μ M (Hill coefficient $n_H = 0.66 \pm 0.23$; $n=2-5$), revealing a 4.1-fold reduction of receptor sensitivity compared to hERG wild-type channels.

In addition to pharmacological hERG current inhibition, we observed impaired hERG cell surface expression after short-term application of desipramine (30 μ M; Fig. 5c).

hERG channels are synthesized in two forms, an immature core glycosylated protein of ~ 135 kDa that is localized in the ER and a fully glycosylated mature form of ~ 155 kDa which is transported to the cell surface (Zhou et al. 1998a, b; Petrecca et al. 1999; Gong et al. 2002; Ficker et al. 2003; Thomas et al. 2003; Staudacher et al. 2010). Compared to drug-free conditions, the amount of mature hERG protein (155 kDa band) was significantly reduced by $28.7 \pm 3.9\%$ (30 min), by $24.9 \pm 5.8\%$ (60 min), and by $37.3 \pm 9.9\%$ (120 min), respectively ($n=6$; Fig. 5d, filled columns). Immature, core glycosylated hERG protein was not significantly affected by desipramine treatment (Fig. 5d, open columns). To compare acute reduction of hERG surface protein to a well-characterized inhibitor of hERG forward trafficking, pentamidine, a chemiluminescence assay was used (Kuryshv et al. 2005; Wible et al. 2005). HEK 293 cells were transfected with hERG WT carrying an

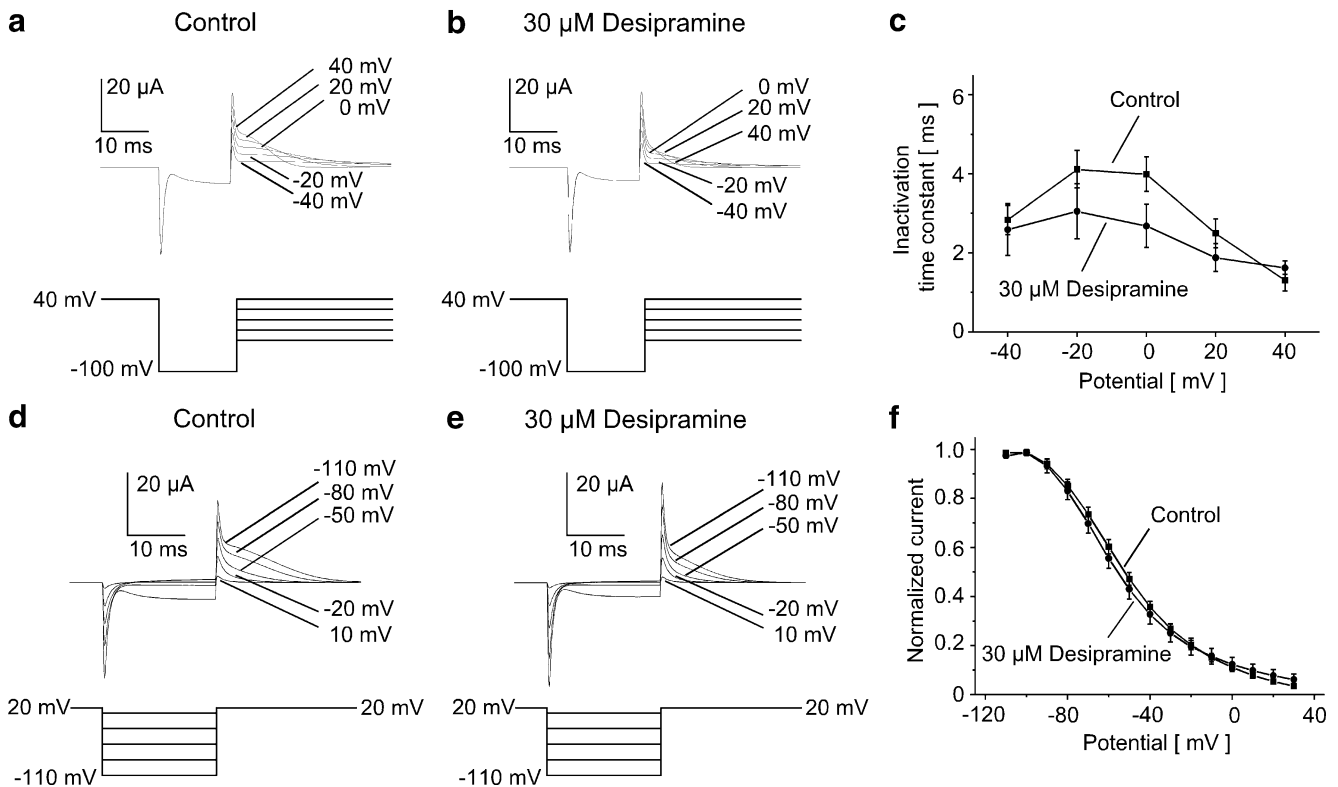


Fig. 4 Desipramine does not modify hERG current inactivation. **a–c** Inactivation time constants were assessed from the third step of the following voltage protocol. Currents were activated by 900 ms pulses to 40 mV, followed by a brief repolarization to -100 mV (16 ms). Variable voltage steps ranging from -40 to 40 mV (150 ms; increment 20 mV) were then applied to evoke inactivating currents (**a, b**). Current measurements recorded from representative oocytes under control conditions (**a**) and after incubation with 30 μ M desipramine (**b**) are displayed. **c** Mean inactivation time constants obtained from

single exponential fits to inactivating current traces ($n=5$). **d, e** Representative single measurements of the steady state inactivation at constant 20 mV after various potentials from -110 to 30 mV (increment 10 mV). For clarity, not all original current traces are displayed. Normalized mean inactivating current amplitudes at 20 mV are shown in **f**, giving steady state inactivation curves. The mean half maximal inactivation voltage was not significantly shifted ($n=5$). Data are given as mean \pm SEM

extracellular HA epitope tag inserted in the extracellular S1–S2 loop (hERG WT HA_{ex}). Insertion of the epitope affects neither electrophysiology nor trafficking of the hERG protein (Ficker et al. 2003). Desipramine (30 μ M) reduced the amount of hERG WT protein at the cell surface ($n=4$; Fig. 5e), confirming the results obtained from Western blots. In contrast, 30 μ M pentamidine induced a weaker effect on hERG surface protein upon short-term drug application after 120 min ($n=4$; Fig. 5e), illustrating that different mechanisms account for acute and chronic drug-induced reductions of the hERG surface protein.

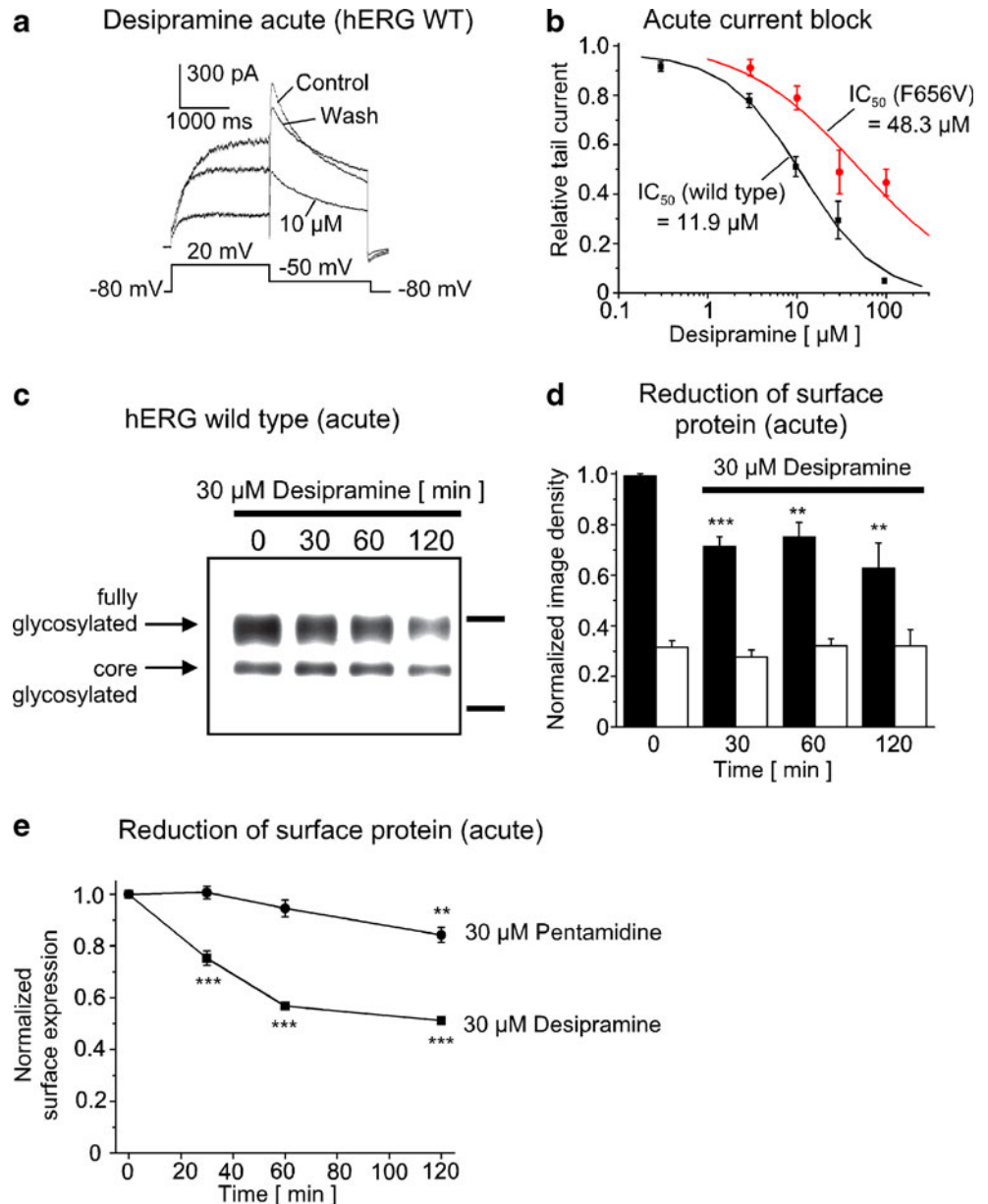
Chronic effects of desipramine: disruption of hERG forward trafficking

hERG ligands have been revealed to decrease cardiac I_{Kr} chronically through impairment of forward protein trafficking to the cell surface (Staudacher et al. 2010). To analyze desipramine-induced chronic changes in cell surface expression, we exposed HEK-hERG WT cells overnight to

increasing concentrations of desipramine and tested for effects on hERG protein processing using Western blot analysis. Incubation with desipramine produced a concentration-dependent decrease in the amount of mature, fully glycosylated hERG protein (Fig. 6a). Changes in surface expression were then quantified using the chemiluminescence assay (Wible et al. 2005). Consistent with the results obtained from Western blots, desipramine caused a significant reduction of surface hERG protein with an IC_{50} value of 17.3 ± 1.1 μ M and a Hill coefficient n_H of 1.54 ± 1.33 ($n=3$ independent assays; Fig. 6c).

To verify our biochemical results, we determined the subcellular localization of hERG protein in the presence of desipramine by anti-hERG immunostaining of stably transfected HEK-hERG cells. Following overnight incubation with 30 μ M desipramine, strong perinuclear staining was observed, indicating accumulation of immature hERG protein in the ER (Fig. 6d). In contrast, non-treated control cells displayed staining of the plasma membrane, consistent with intact trafficking of hERG channels to the cell surface.

Fig. 5 Acute effects of desipramine in mammalian cells. **a** Whole cell patch clamp recordings of HEK 293 cells stably expressing hERG under control conditions, after application of 10 μ M desipramine, and following drug washout. **b** Concentration response curve for acute inhibition of hERG wild type and hERG F656V peak tail currents in HEK 293 cells, giving IC_{50} values of 11.9 and 48.3 μ M, respectively. **c** Western blot, illustrating the effects of short term exposure (30 to 120 min) to 30 μ M desipramine on hERG surface protein. *Upper marker*, 150 kDa; *lower marker*, 100 kDa. **d** Corresponding image density data of fully glycosylated (*filled columns*) and core glycosylated hERG protein (*open columns*), normalized to fully glycosylated protein under drug free conditions. A significant reduction of mature hERG protein at the cell surface after treatment with desipramine is revealed ($n=6$ for each condition). **e** hERG surface protein assessed using a chemiluminescence assay, illustrating significant reduction of protein levels at the cell surface upon short term application of desipramine ($n=4$). Pentamidine, a typical inhibitor of hERG forward trafficking, was markedly less effective ($n=4$). Values were normalized to untreated controls. Data are given as mean \pm SEM; ** $P<0.01$; *** $P<0.001$ versus respective drug free controls



To match the perinuclear staining resulting from desipramine treatment with the subcellular ER compartment, we performed additional labeling using anti-KDEL antibodies that recognize a KDEL retention signal expressed on various ER-resident chaperones (Ficker et al. 2003). Desipramine-associated ER retention of hERG protein was confirmed by overlapping staining patterns produced with anti-hERG and anti-KDEL antibodies (Fig. 6d).

Chronic impairment of hERG cell surface expression resulted in reduced macroscopic current amplitudes. Pulses were applied for 2 s to voltages between -60 and $+80$ mV in 20 mV increments (0.1 Hz), and tail currents were analyzed during a constant repolarizing step to -50 mV for 2 s. Families of hERG current traces from one cell are shown for control conditions and after a 24-h exposure to

30 μ M desipramine (Fig. 6e). The IC_{50} for chronic peak tail current reduction was 7.5 ± 0.2 μ M (Hill coefficient $n_H = 2.36 \pm 0.14$; $n=6-16$ cells; Fig. 6f), similar to the IC_{50} obtained for acute hERG block (11.9 μ M) and for inhibition of surface protein expression (17.3 μ M). One possible explanation for similar drug sensitivities is that desipramine targets a drug-binding site responsible for channel block and impairment of protein trafficking. Substitution of an aromatic phenylalanine residue (F656) inside the hERG ion conducting pore with valine reduced sensitivity to acute hERG blockade significantly (Fig. 5b). In contrast, Western blot and chemiluminescence analyses of mutant hERG F656V and hERG F656V HA_{ex} protein carried out as described above revealed protein trafficking inhibition with similar potency compared to hERG WT.

The desipramine-induced decrease in the amount of fully glycosylated hERG F656V (Fig. 6b) was similar compared to wild-type protein. The reduction of surface hERG F656V protein displayed an IC_{50} value of $20.3 \pm 5.3 \mu M$ and a Hill coefficient n_H of 1.34 ± 0.52 ($n=4$ assays; Fig. 6c). Thus, alteration of F656 did not affect desipramine-induced disruption of hERG protein trafficking, suggesting different mechanisms for acute block and for inhibition of protein trafficking, respectively.

To further explore the mechanism of chronic hERG trafficking block, we attempted to correct drug-induced hERG trafficking inhibition using a pharmacological chaperone. The hERG blocker astemizole has been shown to restore trafficking deficiency induced by digoxin while not affecting hERG WT protein maturation when applied alone (Wang et al. 2009). HEK-hERG WT cells were exposed overnight to $30 \mu M$ desipramine, and astemizole was applied simultaneously at increasing concentrations (10–1,000 nM). The effects on hERG surface protein expression were quantified using Western blot analysis (Fig. 6g). Application of astemizole resulted in concentration-dependent recovery of misprocessed hERG protein with an EC_{50} of 297 ± 24 nM ($30 \mu M$ desipramine; $n=3$ assays). Maximum recovery of fully glycosylated hERG protein was 24.7% (1 μM astemizole). These data provide additional evidence for independent mechanisms underlying acute current inhibition and chronic impairment of protein trafficking.

Desipramine inhibits ERG maturation and suppresses I_{Kr} in HL-1 cardiac myocytes

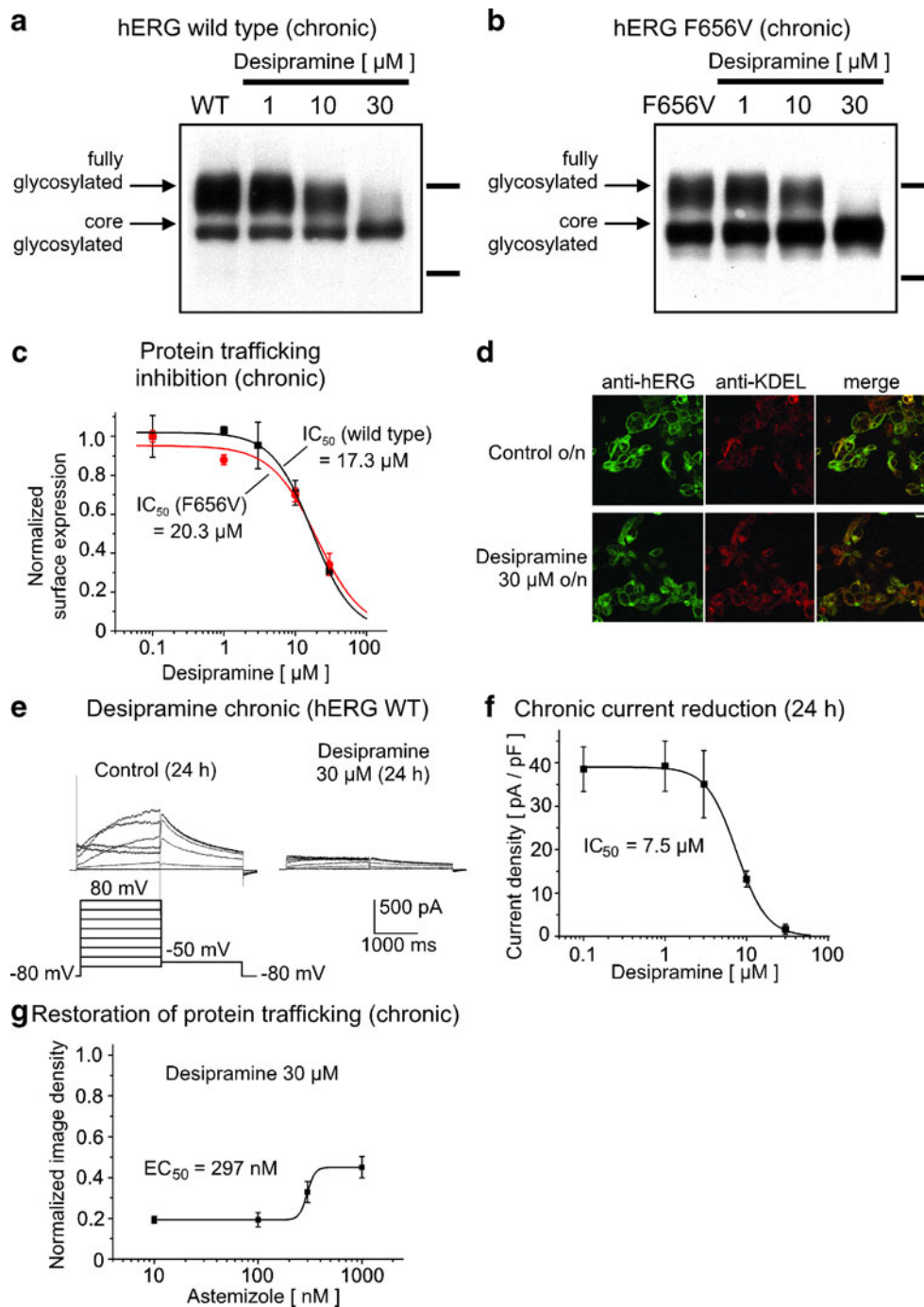
The chronic effects of desipramine on native ERG protein and I_{Kr} current were studied in murine HL-1 cardiac myocytes that exhibit a significant functional endogenous ERG expression (Claycomb et al. 1998). This approach allowed for analysis of ERG protein in a native setting, preventing any bias that may be caused by heterologous gene expression and associated changes in intracellular protein content and trafficking. To assess desipramine-induced inhibition of channel surface expression in HL-1 cells, desipramine (1–30 μM) was applied overnight before ERG protein processing was studied by Western blot analysis. Desipramine produced concentration-dependent suppression of fully glycosylated ERG protein (Fig. 7a), resembling the findings obtained in HEK 293 cells. Reduction of cell surface ERG protein was associated with suppression of the corresponding native ion current, I_{Kr} , as expected (Fig. 7b). Potassium currents were evoked using the protocol described above (Fig. 6e). The tail current component that was activated during the repolarizing voltage step to -50 mV specifically reflects ERG-mediated I_{Kr} (see arrows in Fig. 7b), whereas outward currents are composed of I_{Kr} and additional K^+ conductan-

Fig. 6 Chronic desipramine actions on mammalian cells. **a, b** ▶ Desipramine inhibits maturation and surface expression of hERG protein. Western blot analyses of hERG wild type (**a**) and mutant F656V (**b**) channel protein expressed in HEK 293 cells with overnight exposure to increasing concentrations of desipramine are displayed. *Upper marker*, 150 kDa; *lower marker*, 100 kDa. **c** Surface expression levels determined by chemiluminescence measurements and normalized relative to untreated controls, illustrating concentration dependent reduction of cell surface hERG wild type and hERG F656V protein after overnight exposure to desipramine. The IC_{50} for inhibition of hERG protein trafficking was $17.3 \mu M$ (wild type) and $20.3 \mu M$ (F656V), respectively. **d** Subcellular immunolocalization of hERG wild type protein. HEK hERG cells were fixed and subjected to confocal laser scan microscopy after double labeling with rabbit anti hERG antibody and mouse anti KDEL antibody which was used to indicate endoplasmic reticulum (ER). In untreated control cells, hERG was localized at the cell surface and in the ER. Following overnight treatment with $30 \mu M$ desipramine, hERG resided mostly in the ER, indicating disruption of protein trafficking into the cell surface membrane (*scale bar*, 18 μm). **e** Prolonged exposure to desipramine suppresses I_{hERG} expressed in HEK 293 cells. Representative current recordings obtained under control conditions (*left panel*) and from cells treated overnight with $30 \mu M$ desipramine (*right panel*) are displayed. **f** Corresponding concentration dependence of chronic desipramine treatment on I_{hERG} , revealing an IC_{50} value of $7.5 \mu M$. **g** Restoration of drug induced hERG trafficking block by the pharmacological chaperone, astemizole. Quantification of fully glycosylated cell surface hERG assessed by Western blot after overnight exposure to $30 \mu M$ desipramine and increasing concentrations of astemizole. Maximum protein recovery by astemizole was 24.7% with an EC_{50} value of 297 nM. Data are given as mean \pm SEM

ces, I_K . Mean I_{Kr} tail current density was reduced by 65.4% from 7.8 ± 1.0 pA/pF ($n=12$) after overnight culture in control medium to 2.7 ± 0.6 pA/pF ($n=10$) in the presence of $10 \mu M$ desipramine (Fig. 7c). I_{Kr} was then blocked by application of $5 \mu M$ E4031, and residual I_K was analyzed at the end of the depolarizing pulse to 60 mV. In contrast to I_{Kr} , I_K was not significantly affected by chronic application of $10 \mu M$ desipramine (control medium, 9.0 ± 2.7 pA/pF ($n=9$); desipramine, 6.6 ± 2.4 pA/pF ($n=7$); Fig. 7d).

Cardiac action potential prolongation associated with acute and long-term desipramine treatment

To validate whether the observed in vitro actions of desipramine are relevant to cardiac electrophysiology, the effects of the drug on action potentials recorded from isolated guinea pig ventricular myocytes were studied. Desipramine (1 and $10 \mu M$) was applied acutely until steady-state conditions were achieved, resulting in prolongation of APD_{100} from 223.8 ± 10.1 ms ($n=5$) in the absence of the drug to 277.2 ± 16.7 ms (1 μM ; $n=5$) and to 346.6 ± 20.5 ms ($10 \mu M$; $n=5$) after desipramine exposure, respectively (Fig. 8a, b). Long-term drug effects on action potentials were studied by culturing myocytes overnight in the absence or presence of $30 \mu M$ desipramine. After chronic desipramine treatment, we observed a tendency towards APD_{100} prolongation from $357.9 \pm$



18.2 ms ($n=7$) to 394.8 ± 55.2 ms ($n=6$) (Fig. 8c). This difference, however, did not reach statistical significance. In summary, these results indicate that desipramine administration induces cardiac action potential changes compatible with clinically observed QT prolongation and ventricular tachycardia.

The role of cardiac ERG/ I_{Kr} currents in chronic desipramine-associated APD prolongation was investigated in more detail. A specific inhibitor of ERG channels, E4031, was used to evaluate the contribution of ERG currents to

cardiac repolarization under control conditions and after overnight exposure to 30 μM desipramine. Compared to control cells (mean $\text{APD}_{100} = 357.9$ ms; see above), virtually complete suppression of I_{Kr} by E4031 (5 μM) significantly prolonged APD_{100} to 462.6 ± 24.1 ms ($n=7$) after overnight treatment. In contrast, the APD-prolonging effect of E4031 was attenuated ($\text{APD}_{100} = 422.4 \pm 57.9$ ms; $n=5$) in desipramine-treated myocytes with already delayed repolarization (Fig. 8c). A significant reduction of relative APD prolongation from $29.8 \pm 5.6\%$ (E4031 alone) to $6.4 \pm 5.5\%$ in

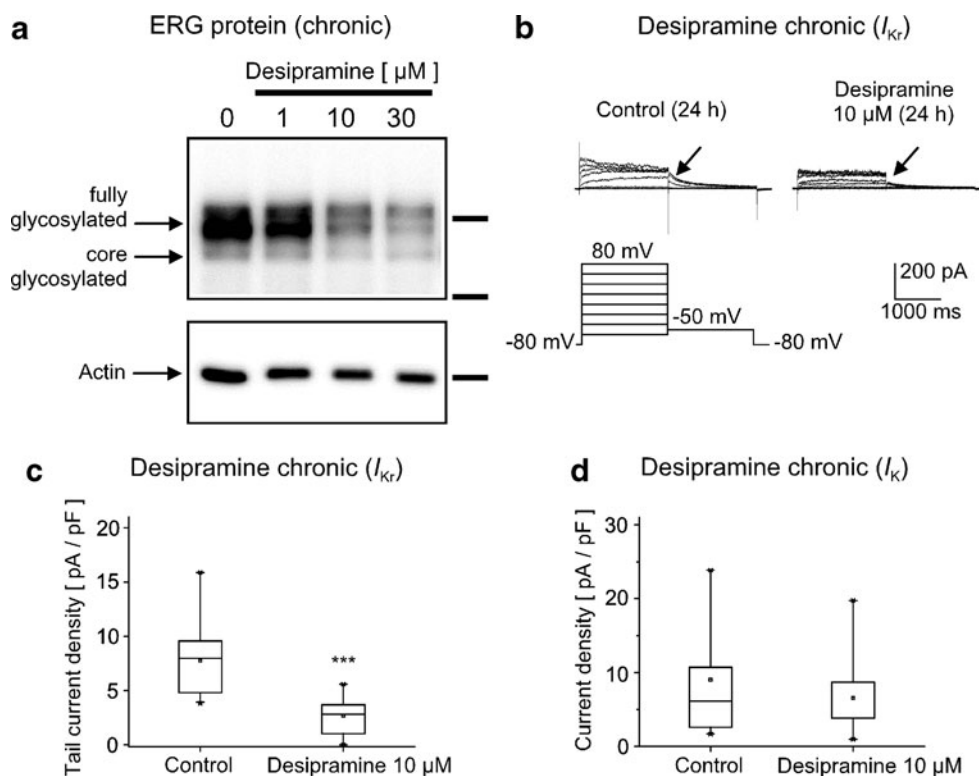


Fig. 7 Chronic effects of desipramine on ERG protein and on I_{K_r} in HL 1 cardiomyocytes. **a** Overnight application of desipramine inhibits trafficking of endogenous murine ERG protein (*upper panel*; 10 μ g protein lysate per lane; *upper marker*, 150 kDa; *lower marker*, 100 kDa). Actin served as loading control (*lower panel*; 5 μ g protein lysate per lane; *marker*, 50 kDa). **b** Chronic exposure to desipramine suppresses native I_{K_r} in HL 1 cardiac myocytes. Representative current recordings obtained under control conditions (*left panel*) and from cells treated overnight with 10 μ M desipramine (*right panel*) are shown. Tail currents that specifically reflect I_{K_r} are indicated by *arrows*. **c**, **d** Quantitative analysis of desipramine effects on I_{K_r} and on total potassium outward current (I_K). Data are represented by

statistical box charts with asterisks representing outliers, whiskers determining the 5th and 95th percentiles, and boxes illustrating the 25th and 75th percentiles (middle bands indicate median). Means are represented by squares. **c** Peak I_{K_r} tail currents recorded during the repolarizing voltage step to -50 mV were significantly reduced by 10 μ M desipramine ($n=10$) compared to recordings obtained under drug free conditions ($n=12$). **d** E4031 resistant outward potassium currents recorded from HL 1 cells during the 60 mV step, reflecting potassium current not mediated by ERG. Mean current amplitudes obtained after overnight application of desipramine ($n=7$) were not significantly different from control currents in the absence of the drug ($n=9$)

the presence of desipramine and E4031 further confirms the common molecular drug target, ERG (Fig. 8d).

Desipramine induces apoptosis

We recently reported apoptotic cell death in association with drugs that inhibit hERG K^+ channels (Thomas et al. 2008; Obers et al. 2010). To assess whether desipramine exerts similar actions, apoptosis was studied in HEK 293 cells. Apoptosis was detected by immunostaining of cleaved PARP (Fig. 9a). PARP is activated in response to DNA damage (Sato and Lindahl 1992). PARP cleavage is a hallmark of apoptosis and allows for differentiation from necrosis. Cells were additionally stained with the nuclear dye, DAPI, and surface-labeled for epithelial cell adhesion molecule (EpCAM) with anti-CD326 antibody. Cells were cultured in drug-free control media or in the presence of 25 μ M desipramine for 5.5 h. Following desipramine

treatment of HEK-hERG cells, we detected significant PARP cleavage indicating apoptosis induction (Fig. 9a; $n=3$ independent assays were performed). In contrast, there was virtually no apoptosis in medium-treated controls or in HEK cells incubated with desipramine (25 μ M). Doxazosin, a hERG inhibitor previously shown to trigger apoptotic cell death in hERG-positive cells (Thomas et al. 2008), served as positive control. Application of 30 μ M doxazosin induced apoptosis of HEK-hERG cells similar to desipramine (Fig. 9a). Desipramine-induced cell death was quantified using an MTT-based cell viability assay. The fraction of viable cells was significantly decreased in HEK-hERG cells treated with 25 μ M desipramine for 22 h ($19.0 \pm 10.7\%$; $n=4$ independent assays) compared to control HEK cells ($37.3 \pm 12.1\%$; $n=4$) (Fig. 9b). The drug concentration applied was sufficient to achieve $\sim 70\%$ hERG current reduction in HEK-hERG cells (Fig. 5b). Application of doxazosin reduced the viability of hERG-positive cells to

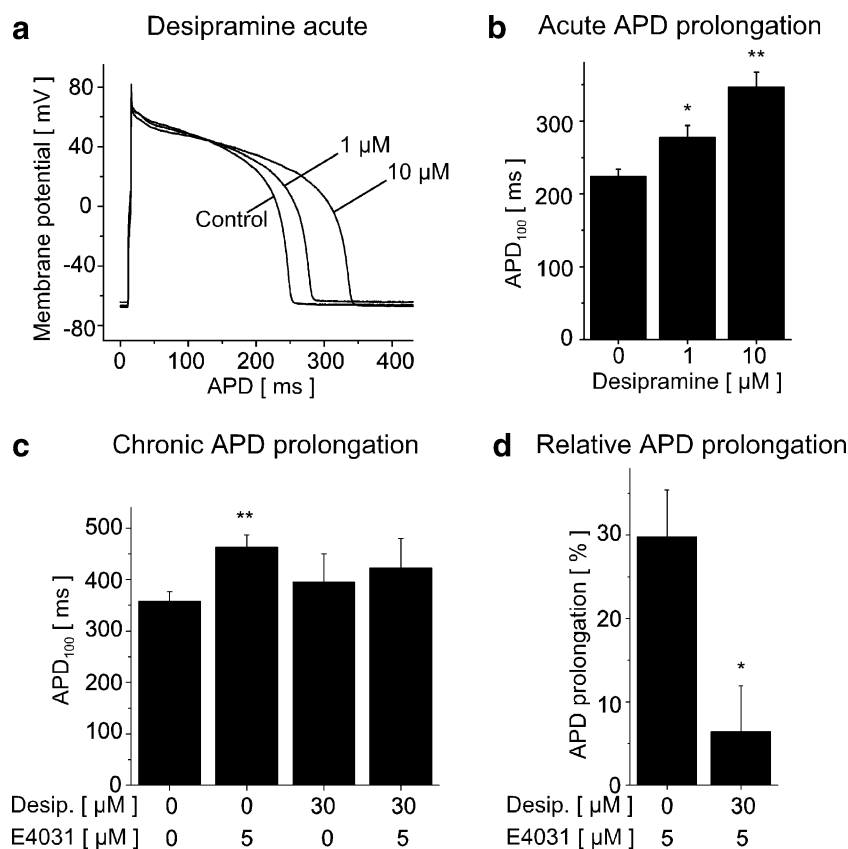


Fig. 8 Cardiac electrophysiology of acute and long term desipramine treatment. **a, b** Acute application of desipramine prolongs the cardiac action potential in freshly isolated guinea pig ventricular myocytes. Representative current clamp recordings of action potentials under control conditions and after extracellular perfusion with desipramine (1 and 10 μM) are displayed in **a**. **b** Quantitative analysis of action potential duration (APD_{100}) recorded in cardiomyocytes upon acute exposure to desipramine. **c** Action potential duration in cardiomyocytes treated overnight with desipramine (30 μM). The specific ERG

inhibitor, E4031 (5 μM), was applied to determine prolongation of cardiac action potentials on blockade of native ERG/ I_{K_r} currents. Chronic hERG reduction by E4031 significantly prolonged APD_{100} only in myocytes cultured without addition of desipramine to the culture media. **d** Relative E4031 associated APD prolongation was significantly reduced by co application of desipramine, indicating that ERG represents the common chronic drug target for both drugs. Data are given as mean \pm SEM. * $P < 0.05$; ** $P < 0.01$ versus respective untreated controls (**a, b**) or versus cells treated with E4031 alone (**d**)

15.6 \pm 6.7% ($n=5$), compared to 49.5 \pm 8.3% ($n=5$) in HEK cells (Fig. 9c).

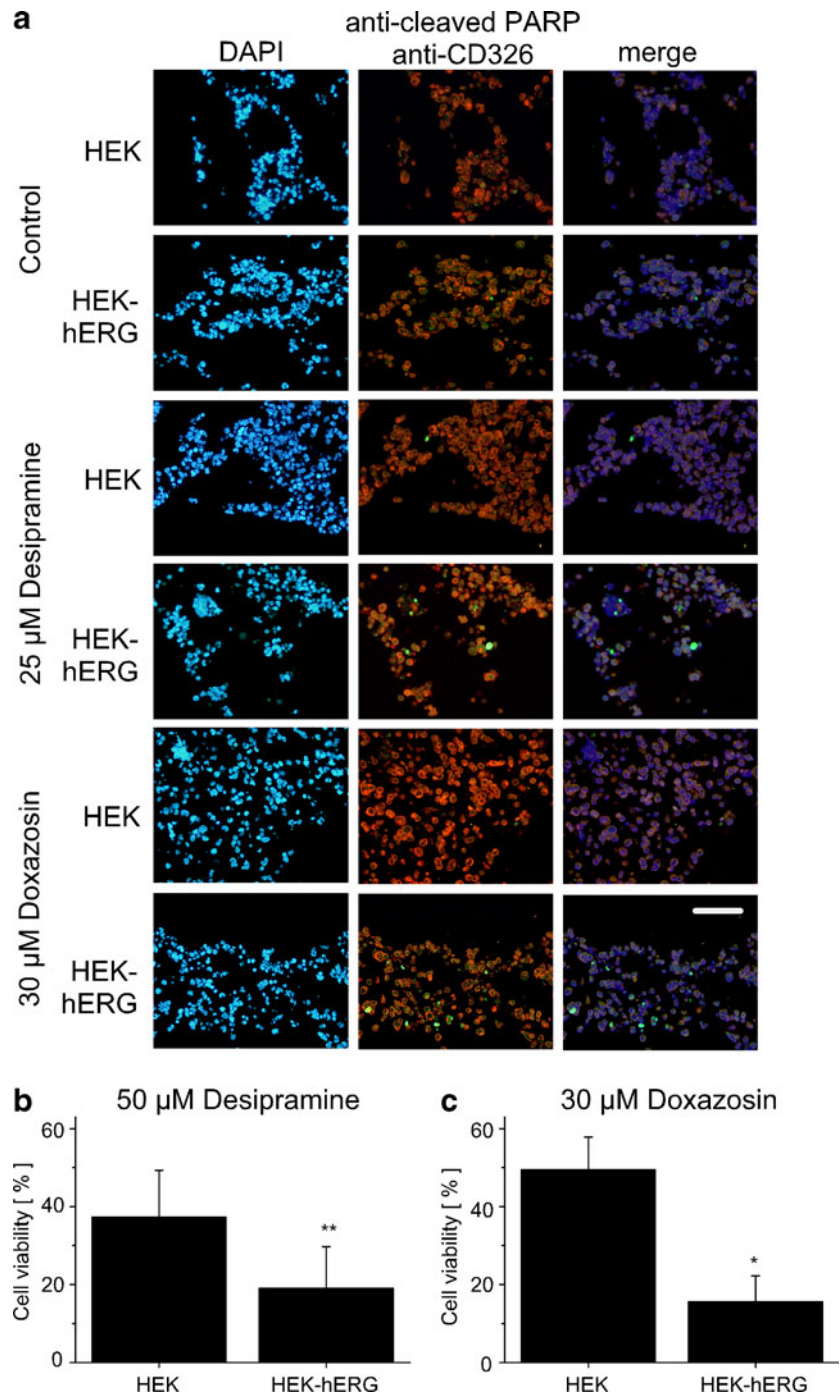
Discussion

Off-target properties account for significant liability of small molecule compounds. Acute hERG current blockade in the heart has been studied extensively as one mechanism underlying drug-induced long QT syndrome. In contrast, the discovery of additional cellular effects associated with hERG potassium channels is ongoing, and their respective molecular pathways are currently less well understood. Here, the tricyclic antidepressant desipramine was used to elucidate the complexity of hERG-related cellular effects. Desipramine has been associated with acquired long QT syndrome and impaired cardiac function, suggesting actions of the drug on cellular electrophysiology and on cell

survival (Burckhardt et al. 1978; Cosazza et al. 1986; Dietrich et al. 1993; Glassmann et al. 1983; Alderton. 1995; Leonard et al. 1995; Swanson et al. 1997; Waslick et al. 1999; Varley 2001).

Multiple potential mechanisms of desipramine-associated hERG liability were assessed. First, we found that hERG K^+ currents were acutely blocked by the antidepressant drug, confirming previous brief reports (Ekins et al. 2002; Wible et al. 2005; Hong et al. 2010). Inhibition of hERG channels expressed in *X. laevis* oocytes displayed an IC_{50} value of 50.1 μM , while hERG currents in HEK 293 cells were inhibited with an IC_{50} of 11.9 μM . This 4.2-fold difference could be readily explained by specific properties of the *Xenopus* oocyte expression system (e.g., the vitelline membrane and the yolk) that presumably reduce the actual concentration of desipramine at the cell surface (Thomas et al. 2001; Obers et al. 2010). In addition, a novel cellular mechanism was detected. Similar to an

Fig. 9 Pro apoptotic effects of desipramine in HEK 293 cells expressing hERG K⁺ channels. **a** Immunolocalization of cells undergoing apoptosis. HEK or HEK hERG cells were analyzed by fluorescence microscopy after staining with anti cleaved PARP antibody (*green*). Mouse anti CD326 (EpCAM) antibody was used in addition as a surface marker of epithelial cells (*red*). Nuclei were visualized by DAPI staining. Apoptosis (green fluorescence) was observed in cells expressing hERG K⁺ channels after treatment with desipramine (25 μ M) similar to the positive control, doxazosin (30 μ M). In contrast, untreated controls and HEK cells after drug incubation exhibited virtually no apoptosis. *Scale bar*, 100 μ m. **b** Cell survival assessed by MTT colorimetric assay (see text for details). HEK or HEK hERG cells were treated with 25 μ M desipramine ($n=4$) or 30 μ M doxazosin ($n=5$) for 22 h. Mean fractions of viable cells (\pm SEM) are shown, illustrating desipramine associated cell death of hERG positive cells ($*P<0.05$; $**P<0.01$). Cell viability after desipramine incubation was normalized to viability of medium treated control HEK or HEK hERG cells, respectively



earlier observation with the antidepressant drug amoxapine (Obers et al. 2010), acute desipramine application significantly reduced the amount of mature hERG protein at the cell surface. Third, long-term desipramine treatment of HEK 293 cells expressing hERG channels resulted in impairment of hERG forward trafficking and reduced surface protein expression ($IC_{50}=17.3 \mu$ M). Thus, desipramine may cause QT prolongation by triple mechanisms, acute ion current blockade, short-term reduction of hERG protein at the cell surface, and long-term disruption of

protein trafficking. Finally, desipramine induced apoptotic cell death of HEK-hERG cells treated with the drug, possibly contributing to heart failure linked to desipramine.

The biophysical mechanism of acute hERG channel blockade by desipramine

The biophysical mechanism of hERG current inhibition was assessed in detail. One important finding of this study is that desipramine blocks hERG channels predominantly in

the open state, as demonstrated using voltage protocols designed to discriminate between open, closed, and inactivated states (Fig. 2). Drug application did not significantly affect biophysics of current activation or inactivation, respectively (Figs. 3 and 4). In oocyte experiments, the mean half-maximal hERG activation voltage ($V_{1/2}$) was 16.6 mV (Fig. 3f). Compared to previous publications (Sanguinetti and Jurkiewicz 1990; Wettwer and Ravens 2005), there are apparent variations of $V_{1/2}$. These differences may result from different voltage protocols or recording conditions (e.g., different bath temperatures during electrophysiological recordings). Voltage protocols that use longer activating voltage steps result in more negative $V_{1/2}$ values as channel activation is time dependent. In addition, the cellular environments of oocytes, mammalian cell lines, and native cardiomyocytes exhibit differences that may affect $V_{1/2}$. Furthermore, regulatory mechanisms such as phosphorylation by protein kinases have been shown to modulate hERG activation (Thomas et al. 2004b). Finally, species-dependent differences in ERG amino acid sequences may account for differential regulation of biophysical properties.

Unblocking upon repolarization, which allows hERG channels to become available for opening, occurred rather slowly, and a complete washout could not be achieved (Fig. 1). As a result, frequency dependence of block was observed (Fig. 2) owing to accumulation of block during channel opening, possibly enhanced by trapping of the drug at its binding site. In a clinical scenario, frequency dependence is expected to produce stronger I_{Kr} inhibition at higher heart rates (i.e., during tachycardia), a mechanism that may exert a beneficial antiarrhythmic effect.

Structural determinants of the hERG drug-binding site as a basis for the high susceptibility of this potassium channel to block by diverse drugs have been revealed. Aromatic rings of amino acid residues Y652 and particularly F656 located in the S6 domain support drug binding (Mitcheson et al. 2000), and mutation of these residues dramatically reduces the potency of several drugs tested to date (for review, see Thomas et al. 2006; Staudacher et al. 2010). Reduced hERG F656V current inhibition by desipramine (Fig. 5) shows that desipramine predominantly binds to this drug receptor within the pore–S6 region. The finding is in line with the work by Hong et al. (2010) showing that drug affinity is reduced in hERG Y652A or hERG F656A. Computational modeling of hERG–desipramine interactions based on these experimental data further illustrates the three-dimensional fit of the drug into the channel pore (Fig. 1).

Short-term drug effects on hERG surface protein

Acute desipramine application (30–120 min) reduced surface expression of hERG channels by 24.9% to 37.3% (Fig. 5). Short-term, drug-induced changes in hERG surface

expression represent a novel finding that we reported very recently for amoxapine (Obers et al. 2010). The half-life for decay of mature hERG protein has been reported to be approximately 10 h in HEK 293 cells (Ficker et al. 2003; Guo et al. 2009). Thus, blockade of forward trafficking can be ruled out as an underlying molecular mechanism. We hypothesize that desipramine may enhance endocytosis and trigger subsequent degradation of hERG protein in an endosomal/lysosomal compartment. Similar pathways have been suggested for hERG protein degradation in response to low extracellular potassium and for Kv1.5 channels upon quinidine binding (Guo et al. 2009; Robertson 2009; Schumacher et al. 2009). Acute reduction of functional hERG protein at the cell surface may contribute to inhibition of macroscopic ionic currents in addition to direct channel blockade. As the underlying molecular mechanism has yet to be resolved, a precise estimation of the relative contribution is not feasible at this time, and further investigation is required in order to fully appreciate its physiological and clinical impact.

Chronic disruption of hERG protein forward trafficking by desipramine

Drug binding to hERG channels may cause I_{Kr} reduction by disruption of hERG protein trafficking into the cell surface membrane, a mechanism that has been reported for several compounds (Staudacher et al. 2010). Drugs may cause acute channel blockade, inhibition of forward trafficking, or both. Chronic desipramine application blocked hERG channel trafficking into the surface membrane in a concentration-dependent manner (IC_{50} = 17.3 μ M), resulting in ER retention of hERG protein and in reduction of macroscopic K^+ currents (IC_{50} = 7.5 μ M; Fig. 6). These observations obtained in a heterologous expression system were extended to cardiac cells. In murine HL-1 cardiomyocytes, desipramine (applied overnight) inhibited maturation of endogenous ERG protein and reduced native I_{Kr} (Fig. 7). Thus, desipramine represents a drug that simultaneously blocks hERG currents and disrupts hERG protein trafficking. Mutation of aromatic pore residue F656 significantly reduced acute hERG inhibition (Fig. 5), while impairment of trafficking was unaffected (Fig. 6), similar to the data reported for the antidepressant drug fluoxetine (Rajamani et al. 2006). In addition, the hERG blocker astemizole was used as pharmacological chaperone. Co-application of astemizole partially restored defective hERG protein trafficking in the presence of desipramine (Fig. 6). Rescue of 65% fully glycosylated hERG protein has previously resulted in 25% I_{hERG} recovery (Wang et al. 2009). Thus, the relatively weak effect detected in this study (i.e., maximum protein increase of ~25%) is not expected to result in significant

hERG current enhancement. In summary, these findings suggest a different interaction site for inhibition of hERG forward trafficking by desipramine compared to acute blockade.

Apoptotic cell death associated with desipramine

Apoptosis induction related to hERG potassium channels has been reported previously for the antihypertensive drug doxazosin, the antidepressant amoxapine, and the antibiotic sparfloxacin (Thomas et al. 2008; Gong et al. 2010; Obers et al. 2010). The rate of apoptosis was significantly increased in hERG-positive cells treated with desipramine (Fig. 9). As the channels are expressed in cardiac myocytes, we may hypothesize that hERG-associated apoptosis contributes to heart failure by progressive cell loss associated with desipramine. Two independent lines of evidence support the hypothesis that apoptosis is mediated by hERG. First, drug-induced apoptosis was observed exclusively in HEK cells expressing hERG channels (Thomas et al. 2008; Obers et al. 2010) (Fig. 9). Second, small interfering RNA-mediated knock-down of hERG in HCT116 colon cancer cells confirmed that apoptosis induction by sparfloxacin required expression of hERG (Gong et al. 2010). Since hERG channels are targeted by multiple drugs, including some that are associated with heart failure, these findings may represent a broader molecular mechanism of hERG-associated cellular side effects. Future studies are required to further validate the significance of this novel mechanism *in vivo*.

Physiological significance: action potential prolongation by desipramine

In contrast to *in vitro* models allowing for a focused assessment of functional and/or biochemical dysregulation of hERG channels, action potential recordings provide an integrated approach to simultaneously evaluate the complex action of desipramine on all cellular factors that contribute to cardiac repolarization. In particular, inhibitory actions of desipramine on L-type calcium or sodium currents are incorporated (Lenkey et al. 2006; Zahradnik et al. 2008). The significance of ERG channel inhibition by desipramine was demonstrated using freshly isolated guinea pig ventricular cardiomyocytes. Acute application of desipramine significantly prolonged the cardiac action potential in a concentration-dependent fashion (Fig. 8). Chronic desipramine exposure and associated impairment of ERG forward trafficking resulted in cardiac action potential prolongation that did not reach statistical significance under the given experimental conditions (Fig. 8). Nonetheless, the contribution of desipramine in long-term APD prolongation was clearly demonstrated by pharmacological competition

with a specific inhibitor of hERG channels, E4031. The APD-prolonging effect of E4031 was significantly attenuated upon simultaneous overnight treatment with desipramine, confirming the common molecular target, cardiac ERG/ I_{Kr} . These mechanisms are expected to result in acute and chronic acquired long QT syndromes, respectively.

Cardiovascular safety of desipramine

Redfern et al. (2003) suggested that a 30-fold safety margin between free drug concentration and experimental IC_{50} value obtained from mammalian cells may indicate proarrhythmic safety of a drug. Drug plasma concentrations range from 0.32 to 3.4 μM after desipramine application (Bertschy et al. 1989; Biederman et al. 1989; Sindrup et al. 1990), and desipramine concentrations between 0.09 and 1.15 μM are observed during imipramine therapy (Brosen et al. 1986). Since desipramine is approximately 90% plasma bound, effective free drug concentrations are ~10-fold lower. The calculated desipramine safety factor ranges from 35 to 371, suggesting a low proarrhythmic potential during therapeutic drug use. Since depression is often associated with suicide attempts, cardiac safety of antidepressant compounds should extend to drug overdose. Desipramine plasma concentrations as high as 6.1 μM have been reported in cases of overdose (Sawyer et al. 1984), resulting in a free drug concentration of 0.61 μM and a safety factor of 20 that indicates clinical significance. In addition, the IC_{50} for chronic trafficking inhibition (17.3 μM) was similar compared to acute current block (11.9 μM), supporting the hypothesis that both mechanisms contribute to prolongation of QT interval associated with arrhythmia in humans. It is noteworthy that the rather benign profile of moderate APD prolongation, frequency dependence, and low risk of proarrhythmia may support antiarrhythmic effects (i.e., suppression of non-sustained ventricular tachycardia and decreased ventricular ectopic depolarization frequency) observed during desipramine treatment (Fenster et al. 1989).

Clinical implications of desipramine-associated cellular effects

In humans during clinical use of the drug, desipramine has been reported to cause QT interval prolongation, torsade de pointes tachycardia, and sudden death, in particular in children and adolescents where desipramine is a commonly prescribed antidepressant (Cosazza et al. 1986; Alderton 1995; Leonard et al. 1995; Swanson et al. 1997; Waslick et al. 1999; Varley 2001; Blair et al. 2004). It should be noted that QT prolongation is not always associated with torsade de pointes. Shah and Hondeghem proposed a more refined indicator for drug-induced proarrhythmia

(Shah and Hondeghem 2005). Recognizing that increased QT intervals may be beneficent or harmful, they combined potential proarrhythmic factors into a proarrhythmic substrate termed TRIaD (*triangulation, reverse use dependence, electrical instability of the action potential, and dispersion*). According to this model, QT prolongation is likely to induce clinical arrhythmia when associated with the presence or augmentation of TRIaD (Dhein et al. 2008; Hondeghem 2008a, b).

In cases where QT prolongation and ventricular arrhythmia are relatively rare, arrhythmogenesis (or lack thereof) may be explained by a multi-hit mechanism that influences repolarization reserve (Witchel et al. 2003). The relatively low proarrhythmic potential of desipramine may in part be attributed to additional calcium channel inhibition by the drug (Zahradnik et al. 2008). A combination of hERG current inhibition and blockade of L-type calcium channels has been suggested to counterbalance action potential prolongation associated with hERG blockers (Thomas et al. 2001), resulting in moderate APD prolongation that was observed in the present study (Fig. 8).

Heart failure, a previously unrecognized potential adverse effect of hERG antagonism, has been linked to desipramine in rare cases (Burckhardt et al. 1978; Glassmann et al. 1983; Dietrich et al. 1993). The development of heart failure may be due to hERG-related pro-apoptotic effects reported here (Fig. 9). As hERG K⁺ channels are expressed in various cancerous cell types, pro-apoptotic action of hERG inhibitors may serve as starting point for the development of anti-cancer drugs (Gong et al. 2010). Future studies are required to close the mechanistic gap between drug binding to hERG channels and initiation of apoptosis.

Conclusion

This study represents a systematic examination of hERG-associated cardiovascular actions of desipramine, assessing four different molecular mechanisms of potential cellular adverse effects. Desipramine-induced QT prolongation caused by acute hERG channel inhibition, by short-term hERG protein reduction, and by disruption of hERG trafficking should be considered to reduce unintended and potentially life-threatening drug side effects. hERG-associated apoptosis is an emerging issue that requires additional investigation. Considering the complex cellular action of desipramine, a need for more refined and efficient methods assessing hERG liability during pharmaceutical drug development is evident.

Acknowledgments We thank William C. Claycomb (New Orleans) for providing HL 1 cells, R. Bloehs for excellent technical support, and H. Erdal for assistance with cell viability assays. This work was

supported in part by grants from the University of Heidelberg and the German Research Foundation (FRONTIERS program to D.T.), the ADUMED Foundation (to D.T.), the German Heart Foundation/German Foundation of Heart Research (to D.T.), the Max Planck Society (TANDEM program to P.A.S.), and the National Institutes of Health (HL71789 to E.F.). W.W. and F.T. acknowledge support from the Landesstiftung Baden Württemberg and the German Research Foundation Center for Functional Nanostructures.

Conflict of interest statement The authors declare that they have no conflict of interest.

References

- Alderton HR (1995) Tricyclic medication in children and the QT interval: case report and discussion. *Can J Psychiatry* 40:325–329
- Bertschy G, Vandel S, Vandel B, Allers G, Bechtel P, Volmat R (1989) Desipramine dose prediction based on 24 hour single dose levels: feasibility and validity. *Pharmacopsychiatry* 22:161–164
- Bianchi L, Wible B, Arcangeli A, Tagliatela M, Morra F, Castaldo P, Crociati O, Rosati B, Faravelli L, Olivotto M, Wanke E (1998) Herg encodes a K⁺ current highly conserved in tumors of different histogenesis: a selective advantage for cancer cells? *Cancer Res* 58:815–822
- Biederman J, Baldessarini RJ, Wright V, Knee D, Hartz J, Goldblatt A (1989) A double blind placebo controlled study of desipramine in the treatment of ADD: II. Serum drug levels and cardiovascular findings. *J Am Acad Child Adolesc Psychiatry* 28:903–911
- Blair J, Taggart B, Martin A (2004) Electrocardiographic safety profile and monitoring guidelines in pediatric psychopharmacology. *J Neural Transm* 111:791–815
- Brosen K, Gram LF, Klysner R, Bech P (1986) Steady state levels of imipramine and its metabolites: significance of dose dependent kinetics. *Eur J Clin Pharmacol* 30:43–49
- Burckhardt D, Raeder E, Müller V, Imhof P, Neubauer H (1978) Cardiovascular effects of tricyclic and tetracyclic antidepressants. *JAMA* 239:213–216
- Cherubini A, Taddei GL, Crociani O, Paglierani M, Buccoliero AM, Fontana L, Noci I, Borri P, Borriani E, Giachi M, Becchetti A, Rosati B, Wanke E, Olivotto M, Arcangeli A (2000) HERG potassium channels are more frequently expressed in human endometrial cancer as compared to non cancerous endometrium. *Br J Cancer* 83:1722–1729
- Claycomb WC, Lanson NA Jr, Stallworth BS, Egeland DB, Delcarpio JB, Bahinski A, Izzo NJ Jr (1998) HL 1 cells: a cardiac muscle cell line that contracts and retains phenotypic characteristics of the adult cardiomyocyte. *Proc Natl Acad Sci USA* 95:2979–2984
- Coccaro EF, Siever LJ (1983) Second generation antidepressants: a comparative review. *J Clin Pharmacol* 25:241–260
- Cordes JS, Sun S, Lloyd DB, Bradley JA, Opsahl AC, Tengowski MW, Chen X, Zhou J (2005) Pentamidine reduces hERG expression to prolong the QT interval. *Br J Pharmacol* 145:12–23
- Cosazza F, Fiorista F, Rustici A, Brambilla G (1986) Torsade de pointes caused by tricyclic antidepressive agents. Description of a clinical case. *G Ital Cardiol* 16:1058–1061
- Crociani O, Guasti L, Balzi M, Becchetti A, Wanke E, Olivotto M, Wymore RS, Arcangeli A (2003) Cell cycle dependent expression of HERG1 and HERG1B isoforms in tumor cells. *J Biol Chem* 278:2947–2955
- Daugherty A, Frayn KN, Redfern WS, Woodward B (1986) The role of catecholamines in the production of ischaemia induced ventricular arrhythmias in the rat in vivo and in vitro. *Br J Pharmacol* 87:265–277

- Dhein S, Perlitz F, Mohr FW (2008) An in vitro model for assessment of drug induced torsade de pointes arrhythmia: effects of haloperidol and dofetilide on potential duration, repolarization inhomogeneities, and torsade de pointes arrhythmia. *Naunyn Schmiedebergs Arch Pharmacol* 378:631 644
- Dietrich A, Mortensen ME, Wheller J (1993) Cardiac toxicity in an adolescent following chronic lithium and imipramine therapy. *J Adolesc Health* 14:394 397
- Du XJ, Woodcock EA, Little PJ, Esler MD, Dart AM (1998) Protection of neuronal uptake 1 inhibitors in ischemic and anoxic hearts by norepinephrine dependent and independent mechanisms. *J Cardiovasc Pharmacol* 32:621 628
- Eisenberg D, McLachlan AD (1986) Solvation energy in protein folding and binding. *Nature* 319:199 203
- Ekins S, Crumb WJ, Sarazan D, Wikel JH, Wrighton SA (2002) Three dimensional quantitative structure activity relationship for inhibition of human ether a go go related gene potassium channel. *J Pharmacol Exp Ther* 301:427 434
- Farid R, Day T, Friesner R, Pearlstein R (2005) New insights about HERG blockade obtained from protein modeling, potential energy mapping, and docking studies. *Bioorg Med Chem* 14:3160 3173
- Fenster PE, Bressler R, Kipps J (1989) Antiarrhythmic efficacy of desipramine. *J Clin Pharmacol* 29:114 117
- Ficker E, Dennis AT, Wang L, Brown AM (2003) Role of cytosolic chaperones Hsp70 and Hsp90 in maturation of the cardiac potassium channel HERG. *Circ Res* 92:e87 e100
- Ficker E, Kuryshv YA, Dennis AT, Obejero Paz C, Wang L, Hawryluk P, Wible BA, Brown AM (2004) Mechanisms of arsenic induced prolongation of cardiac repolarization. *Mol Pharmacol* 66:33 44
- Fischer B, Basili S, Merlitz H, Wenzel W (2007) Accuracy of binding mode prediction with a cascading stochastic tunneling method. *Proteins* 68:195 204
- Glassmann AH, Johnson LL, Giardina EG, Walsh BT, Roose SP, Cooper TB, Bigger JT Jr (1983) The use of imipramine in depressed patients with congestive heart failure. *JAMA* 250:1997 2001
- Gong Q, Anderson CL, January CT, Zhou Z (2002) Role of glycosylation in cell surface expression and stability of HERG potassium channels. *Am J Physiol* 283:H77 H84
- Gong JH, Liu XJ, Shang BY, Chen SZ, Zhen YS (2010) HERG K⁺ channel related chemosensitivity to sparfloxacin in colon cancer cells. *Oncol Rep* 23:1747 1756
- Guo J, Massaeli H, Li W, Xu J, Luo T, Shaw J, Kirshenbaum LA, Zhang S (2007) Identification of I_{Kr} and its trafficking disruption induced by probucol in cultured neonatal rat cardiomyocytes. *J Pharmacol Exp Ther* 321:911 920
- Guo J, Massaeli H, Xu J, Jia Z, Wigle JT, Mesaali N, Zhang S (2009) Extracellular K⁺ concentration controls cell surface density of I_{Kr} in rabbit hearts and of the HERG channel in human cell lines. *J Clin Invest* 119:2745 2757
- Hondeghem LM (2008a) QT prolongation is an unreliable predictor of ventricular arrhythmia. *Heart Rhythm* 5:1210 1212
- Hondeghem LM (2008b) Use and abuse of QT and TRiA in cardiac safety research: importance of study design and conduct. *Eur J Pharmacol* 584:1 9
- Hong HK, Park MH, Lee BH, Jo SH (2010) Block of the human ether a go go related gene (hERG) K⁺ channel by the antidepressant desipramine. *Biochem Biophys Res Commun* 394:536 541
- Jiang Y, Lee A, Chen J, Ruta V, Cadene M, Chait BT, MacKinnon R (2003) X ray structure of a voltage gated K⁺ channel. *Nature* 423:33 41
- Jorgensen WL, McDonald NA (1997) Development of an all atom force field for heterocycles. Properties of liquid pyridine and diazenes. *J Mol Struct* 424:145 155
- Kiehn J, Thomas D, Karle CA, Schöls W, Kübler W (1999) Inhibitory effects of the class III antiarrhythmic drug amiodarone on cloned HERG potassium channels. *Naunyn Schmiedebergs Arch Pharmacol* 359:212 219
- Kokh DB, Wenzel WG (2008) Flexible side chain models improve enrichment rates in in silico screening. *J Med Chem* 51:5919 5931
- Kuryshv YA, Ficker E, Wang L, Hawryluk P, Dennis AT, Wible BA, Brown AM, Kang J, Chen XL, Sawamura K, Reynolds W, Rampe D (2005) Pentamidine induced long QT syndrome and block of hERG trafficking. *J Pharmacol Exp Ther* 312:316 323
- Kurz T, Offner B, Schreieck J, Richardt G, Tölg R, Schömig A (1995) Nonexocytotic noradrenaline release and ventricular fibrillation in ischemic rat hearts. *Naunyn Schmiedebergs Arch Pharmacol* 352:491 496
- Lenkey N, Karoly R, Kiss JP, Szasz BK, Vizi ES, Mike A (2006) The mechanism of activity dependent sodium channel inhibition by the antidepressants fluoxetine and desipramine. *Mol Pharmacol* 70:2052 2063
- Leonard HL, Meyer MC, Swedo SE, Richter D, Hamburger SD, Allen AJ, Rapoport JL, Tucker E (1995) Electrocardiographic changes during desipramine and clomipramine treatment in children and adolescents. *J Am Acad Child Adolesc Psychiatry* 34:1460 1468
- Merlitz H, Wenzel W (2002) Comparison of stochastic optimization methods for receptor ligand docking. *Chem Phys Lett* 362:271 277
- Merlitz H, Burghardt B, Wenzel W (2003) Application of the stochastic tunneling method to high throughput database screening. *Chem Phys Lett* 370:68 73
- Mitcheson JS, Chen J, Lin M, Culberson C, Sanguinetti MC (2000) A structural basis for drug induced long QT syndrome. *Proc Natl Acad Sci USA* 97:12329 12333
- Morita H, Wu J, Zipes DP (2008) The QT syndromes: long and short. *Lancet* 372:750 763
- Morris GM, Goodsell DS, Halliday R, Huey R, Hart WE, Belew RK, Olson AJ (1998) Automated docking using a Lamarckian genetic algorithm and an empirical binding free energy function. *J Comput Chem* 19:1639 1662
- Mosmann T (1983) Rapid colorimetric assay for cellular growth and survival: application to cytotoxic and survival assays. *J Immunol Methods* 65:55 63
- Obers S, Staudacher I, Ficker E, Dennis A, Koschny E, Erdal H, Bloehs R, Kisselbach J, Karle CA, Schweizer PA, Katus HA, Thomas D (2010) Multiple mechanisms of hERG liability: K⁺ current inhibition, disruption of protein trafficking, and apoptosis induced by amoxapine. *Naunyn Schmiedebergs Arch Pharmacol* 381:385 400
- Petrecca K, Atanasiu R, Akhavan A, Shrier A (1999) N linked glycosylation sites determine HERG channel surface membrane expression. *J Physiol* 515:41 48
- Rajamani S, Eckhardt LL, Valdivia CR, Klemens CA, Gillman BM, Anderson CL, Holzem KM, Delisle B, Anson BD, Makielski JC, January CT (2006) Drug induced long QT syndrome: hERG K⁺ channel block and disruption of protein trafficking by fluoxetine and norfluoxetine. *Br J Pharmacol* 149:481 489
- Redfern WS, Carlsson L, Davis AS, Lynch WG, MacKenzie I, Palethorpe S, Siegl PK, Strang I, Sullivan AT, Wallis R, Camm AJ, Hammond TG (2003) Relationships between preclinical cardiac electrophysiology, clinical QT interval prolongation and torsade de pointes for a broad range of drugs: evidence for a provisional safety margin in drug development. *Cardiovasc Res* 58:32 45
- Robertson GA (2009) Endocytic control of ion channel density as a target for cardiovascular disease. *J Clin Invest* 119:2531 2534
- Roden D (2008) Repolarization reserve: a moving target. *Circulation* 118:981 982

- Sanguinetti MC, Jurkiewicz NK (1990) Two components of cardiac delayed rectifier K⁺ current. Differential sensitivity to block by class III antiarrhythmic agents. *J Gen Physiol* 96:195-215
- Sanguinetti MC, Tristani Firouzi M (2006) hERG potassium channels and cardiac arrhythmia. *Nature* 440:463-469
- Sanguinetti MC, Jiang C, Curran ME, Keating MT (1995) A mechanistic link between an inherited and an acquired cardiac arrhythmia: HERG encodes the I_{Kr} potassium channel. *Cell* 81:299-307
- Satoh MS, Lindahl T (1992) Role of poly (ADP ribose) formation in DNA repair. *Nature* 356:356-358
- Sawyer WT, Caudill JL, Ellison MJ (1984) A case of severe acute desipramine overdose. *Am J Psychiatry* 141:122-123
- Schumacher SM, McEwen DP, Zhang L, Arendt KL, Van Genderen KM, Martens JR (2009) Antiarrhythmic drug induced internalization of the atrial specific K⁺ channel Kv1.5. *Circ Res* 104:1390-1398
- Shah RR, Hondeghem LM (2005) Refining detection of drug induced proarrhythmia: QT interval and TRIaD. *Heart Rhythm* 2:758-772
- Sindrup SH, Gram LF, Skjold T, Grodum E, Brosen K, Beck Nielsen H (1990) Clomipramine vs. desipramine vs. placebo in the treatment of diabetic neuropathy symptoms. A double blind cross over study. *Br J Clin Pharmacol* 30:683-691
- Smith GAM, Tsui HW, Newell EW, Jiang X, Zhu XP, Tsui FWL, Schlichter LC (2002) Functional up regulation of HERG K⁺ channels in neoplastic hematopoietic cells. *J Biol Chem* 277:18528-18534
- Staudacher I, Schweizer PA, Katus HA, Thomas D (2010) hERG: protein trafficking and potential for drug side effects. *Curr Opin Drug Discov Dev* 13:23-30
- Swanson JR, Jones GR, Krasselt W, Denmark LN, Ratti F (1997) Death of two subjects due to imipramine and desipramine metabolite accumulation during chronic therapy: a review of the literature and possible mechanisms. *J Forensic Sci* 42:335-339
- Takemasa H, Nagatomo T, Abe H, Kawakami K, Igarashi T, Tsuguri T, Kabashima N, Tamura M, Okazaki M, Delisle BP, January CT, Otsuji Y (2007) Coexistence of hERG current block and disruption of protein trafficking in ketoconazole induced long QT syndrome. *Br J Pharmacol* 153:439-447
- The ALLHAT Officers and Coordinators for the ALLHAT Collaborative Research Group (2000) Major cardiovascular events in hypertensive patients randomized to doxazosin vs chlorthalidone: the Antihypertensive and Lipid Lowering Treatment to Prevent Heart Attack Trial (ALLHAT). *JAMA* 283:1967-1975
- Thomas D, Zhang W, Karle CA, Kathöfer S, Schöls W, Kübler W, Kiehn J (1999) Deletion of protein kinase A phosphorylation sites in the HERG potassium channel inhibits activation shift by protein kinase A. *J Biol Chem* 274:27457-27462
- Thomas D, Wendt Nordahl G, Röckl K, Ficker E, Brown AM, Kiehn J (2001) High affinity blockade of HERG human cardiac potassium channels by the novel antiarrhythmic drug BRL 32872. *J Pharmacol Exp Ther* 297:735-761
- Thomas D, Kiehn J, Katus HA, Karle CA (2003) Defective protein trafficking in hERG associated hereditary long QT syndrome (LQT2): molecular mechanisms and restoration of intracellular protein processing. *Cardiovasc Res* 60:235-241
- Thomas D, Wimmer AB, Wu K, Hammerling BC, Ficker EK, Kuryshev Y, Kiehn J, Katus HA, Schoels W, Karle CA (2004a) Inhibition of human ether a go go related gene potassium channels by the α 1 adrenoceptor antagonists prazosin, doxazosin, and terazosin. *Naunyn Schmiedeberg Arch Pharmacol* 369:462-472
- Thomas D, Kiehn J, Katus HA, Karle CA (2004b) Adrenergic regulation of the rapid component of the cardiac delayed rectifier potassium current, I(Kr), and the underlying hERG ion channel. *Basic Res Cardiol* 99:279-287
- Thomas D, Karle CA, Kiehn J (2006) The cardiac hERG/I_{Kr} potassium channel as pharmacological target: structure, function, regulation, and clinical applications. *Curr Pharm Des* 12:2271-2283
- Thomas D, Bloehs R, Koschny R, Ficker E, Sykora J, Kiehn J, Schlömer K, Gierten J, Kathöfer S, Zitron E, Scholz EP, Kiesecker C, Katus HA, Karle CA (2008) Doxazosin induces apoptosis of cells expressing hERG potassium channels. *Eur J Pharmacol* 579:98-103
- Van der Heyden MAG, Smits ME, Vos MA (2008) Drugs and trafficking of ion channels: a new pro arrhythmic threat on the horizon? *Br J Pharmacol* 153:406-409
- Varley CK (2001) Sudden death related to selected tricyclic antidepressants in children: epidemiology, mechanisms and clinical implications. *Paediatr Drugs* 3:613-627
- Viskin S (1999) Long QT syndromes and torsade de pointes. *Lancet* 354:1625-1633
- Wang H, Zhang Y, Cao L, Han H, Wang J, Yang B, Nattel S, Wang Z (2002) HERG K⁺ channel, a regulator of tumor cell apoptosis and proliferation. *Cancer Res* 62:4843-4848
- Wang L, Wible BA, Wan X, Ficker E (2007) Cardiac glycosides as novel inhibitors of human ether a go go related gene channel trafficking. *J Pharmacol Exp Ther* 320:525-534
- Wang L, Dennis AT, Trieu P, Charron F, Ethier N, Hebert TE, Wan X, Ficker E (2009) Intracellular potassium stabilizes human ether a go go related gene channels for export from endoplasmic reticulum. *Mol Pharmacol* 75:927-937
- Warmke JW, Ganetzky B (1994) A family of potassium channel genes related to eag in *Drosophila* and mammals. *Proc Natl Acad Sci USA* 91:3438-3442
- Waslick BD, Walsh BT, Greenhill LL, Giardina EG, Sloan RP, Bigger JT, Bilich K (1999) Cardiovascular effects of desipramine in children and adults during exercise testing. *J Am Acad Child Adolesc Psychiatry* 38:179-186
- Wenzel W, Hamacher K (1999) Stochastic tunneling approach for global optimization of complex potential energy landscapes. *Phys Rev Lett* 82:3003-3007
- Wettwer E, Ravens U (2005) Recording cardiac potassium currents with the whole cell voltage clamp technique. In: Dhein S, Mohr FW, Delmar M (eds) Practical methods in cardiovascular research, 1st edn. Springer, Heidelberg, pp 355-380
- Wible BA, Hawryluk P, Ficker E, Kuryshev YA, Kirsch G, Brown AM (2005) HERG Lite: a novel comprehensive high throughput screen for drug induced hERG risk. *J Pharmacol Toxicol Methods* 52:136-145
- Witchel HJ, Hancox JC, Nutt DJ (2003) Psychotropic drugs, cardiac arrhythmia, and sudden death. *J Clin Psychopharmacol* 23:58-77
- Zahradnik I, Minarovic I, Zahradnikova A (2008) Inhibition of cardiac L type calcium channel current by antidepressant drugs. *J Pharmacol Exp Ther* 324:977-984
- Zhou Z, Gong Q, Epstein ML, January CT (1998a) HERG channel dysfunction in human long QT syndrome: intracellular transport and functional defects. *J Biol Chem* 273:21061-21066
- Zhou Z, Gong Q, Ye B, Fan Z, Makielski JC, Robertson GA, January CT (1998b) Properties of HERG channels stably expressed in HEK 293 cells studied at physiological temperature. *Biophys J* 74:230-241